INL/EXT-10-18973

Vacuum Bellows, Vacuum Piping, Cryogenic Break, and Copper Joint Failure Rate Estimates for ITER Design Use

L. Cadwallader

June 2010

The INL is a U.S. Department of Energy National Laboratory
operated by Battelle Energy Alliance

INL/EXT-10-18973

Vacuum Bellows, Vacuum Piping, Cryogenic Break, and Copper Joint Failure Rate Estimates for ITER Design Use

L. Cadwallader

June 2010

Idaho National Laboratory
Thermal Sciences and Safety Analysis Department
Idaho Falls, Idaho 83415

http://www.inl.gov

Prepared for the
Office of Federal and State Materials and Environmental Management Programs
U.S. Nuclear Regulatory Commission
Washington, DC 20555

ABSTRACT

The ITER international project design teams are working to produce an engineering design in preparation for construction of the International Thermonuclear Experimental Reactor (ITER) tokamak. During the course of this work, questions have arisen in regard to safety barriers and equipment reliability as important facets of system design. The vacuum system designers have asked several questions about the reliability of vacuum bellows and vacuum piping. The vessel design team has asked about the reliability of electrical breaks and copper-copper joints used in cryogenic piping. Research into operating experiences of similar equipment has been performed to determine representative failure rates for these components. The following chapters give the research results and the findings for vacuum system bellows, power plant stainless steel piping (amended to represent vacuum system piping), cryogenic system electrical insulating breaks, and copper joints.

CONTENTS

FIGURES

TABLES

NOMENCLATURE

AL-SS	aluminum-to-stainless steel joint
CERN	European Organization for Nuclear Research
D	deuterium
DN	diametre nominal
DOE	U.S. Department of Energy
EDA	Engineering Design Activity
H	hydrogen, protium
IO	International Organization
ITER	International Thermonuclear Experimental Reactor
JET	Joint European Torus
LEP	Large Electron Positron collider
LHe	liquid helium
RF	radiofrequency
SS	stainless steel
T	tritium
TIG	tungsten inert gas welding
ub	upper bound
UHV	ultra high vacuum
UNS	Unified Numbering System
β	beta factor for common cause failure analysis
χ^2	chi-square statistical distribution

Vacuum Bellows, Vacuum Piping, Cryogenic Break, and Copper Joint Failure Rate Estimates for ITER Design Use

1. INTRODUCTION

The ITER international project design teams are working to produce an engineering design in preparation for construction of the International Thermonuclear Experimental Reactor (ITER) tokamak. During the course of this work, questions have arisen in regard to safety barriers and equipment reliability as important facets of system design. The vacuum system designers have asked several questions about the reliability of vacuum bellows and vacuum piping. The vessel design team has asked about the reliability of electrical breaks and copper-copper joints used in cryogenic piping. Research into operating experiences of similar equipment has been performed to determine representative failure rates for these components. The following chapters give the research results and the findings for vacuum bellows, stainless steel power plant piping (amended to represent vacuum piping), cryogenic system electrical insulating breaks, and copper joints.

2. VACUUM BELLOWS FAILURE RATES

Failure rates for vacuum bellows are of interest to ITER vacuum system designers since it is acknowledged that bellows units are more fragile than vacuum piping. In order to find operating experience-based reliability data on stainless steel bellows that would be applicable to ITER vacuum uses of bellows, the particle accelerator literature was searched. Some quantitative operating experience data from the Large Electron-Positron Collider (LEP) at the European Organization for Nuclear Research (CERN) have been reviewed. The LEP staff published sufficient information to make an initial failure rate estimate for stainless steel bellows in vacuum service on the LEP.

Three key pieces of data are needed for a component failure rate calculation. The first is the component population, that is, the count of components in service that are experiencing the operational environment of interest. Second is the count of the number of units that have failed, including the manner in which they failed. Lastly, the operating time for the set of components is needed. The discussion below quotes these data or makes assumptions about the set of components if such assumptions are warranted. Particle accelerators tend to be good sources of inference failure rates since they operate large numbers of components for significant amounts of time.

2.1 LEP Bellows Count and Engineering Description

The LEP experiment was a large accelerator at the CERN complex, operating from mid-July 1989 to early November 2000. From published engineering data, the LEP standard vacuum bellows were circular cross-section, hydroformed convolution bellows with single walls. Each bellows had 10 convolutions and a 14-mm convolution height (Unterlerchner, 1990). The bellows were constructed of 316L stainless steel (SS). The units were 0.168 m in length and 0.188 m in outer diameter. The bellows wall thickness was 0.15 mm and the bellows on average compressed about 37 mm during LEP bakeout. The bakeout temperature of the LEP sections was 150°C but the bellows units were not directly heated by hot water like the vacuum section aluminum segments, so the bellows units themselves only reached about 50°C during the 24-hour bakeout (Strubin, 1996). The bellows were rated for a radial offset of 3 mm to account for installation and alignment tolerances. The bellows had a design requirement of 250 compression-expansion cycles at bakeout temperature (Unterlerchner, 1990). An additional design requirement was a life of 10,000 cycles of 6 mm stroke at room temperature. Each bellows unit had an inner metallic sleeve for radiofrequency (RF) energy protection. The LEP stainless steel flange bellows used an aluminum gasket to seal to an aluminum flange on the aluminum vacuum chamber 'straight sections' (Unterlerchner, 1990). The aluminum gasket was chosen instead of a copper gasket due to the risk of galvanic corrosion of a copper gasket and an aluminum flange in the presence of nitric acid, which can form outside the accelerator from stray radiation (LEP, 1984). For this assessment, the bellows component includes its flange connections to other vacuum components. The ITER designers noted that these bellows units were bolted flange seals with vacuum gaskets rather than welded connections. Welded connections are qualitatively stated to be the most reliable, long-lived connection in a vacuum environment (O'Hanlon, 2003). Welded connections generally give better leakage performance than bolted flanges, but in this case the LEP had very few leak events, and none of the leaks were specifically attributed to the flange seals.

There were 2,649 standard bellows units in use on the LEP, and another 473 non-standard bellows for a total number of 3,122 units. As a conservatism, only the standard bellows have been considered for the LEP leakage events that occurred on the collider rather than adding in the non-standard bellows units. Most of the reported data on leaks were for standard bellows units. These high numbers of bellows units were necessary because the LEP was a large accelerator, ≈27 km in circumference (Gröbner, 1990). The base vacuum in the aluminum vacuum sections of the accelerator was in the low 1E−08 Pa range, and the vacuum during beam storage was < 4E−07 Pa (LEP, 1990). Thus, the bellows units were under ultra high vacuum (UHV). The typical operating temperature of the walls was not cited in any of the references, so it is assumed to be close to room temperature, on the order of 15-20°C, but excursions to higher temperatures were possible – perhaps up to as high as 60°C (Bryan, 2009). Gröbner (1991) stated that the power loss for LEP was 882 W/m of length; the LEP had a water cooling system to remove that heat.

Many types of LEP vacuum components were subjected to 100% component inspection, testing, and pre-installation cleaning before assembly on the LEP ring (LEP, 1990; Strubin, 1996). However, the bellows were not part of the 100% testing. The bellows received only visual inspection and mandatory cleaning. The LEP specifications stated that a pre-series test of 10 bellows assemblies were carried out for bellows lifetime, mechanical, and vacuum tests (LEP, 1985). During production, factory tests included material quality, dimensional accuracy, elastic properties, leak tightness, fitting and function tests. CERN performed tests of one bellows per batch of 100 production units delivered to CERN. If that bellows failed a test, then a second bellows would be pulled from the batch and tested. If the second bellows failed, that batch would be rejected. If two batches in a row were rejected, production of bellows would stop and the cause for failure would be identified and resolved. The CERN testing of bellows included leak tightness evaluation of a 10-minute helium test at 0.1 MPa, with success indicated by leak rates less than 1E−11 Pa-m^3/s (LEP, 1985). Life testing was carried out under simulated LEP conditions, namely a 150°C bakeout, 37 mm stroke and the 3 mm radial offset between flanges (Gröbner, 1991a). The tested bellows units gave an average lifetime of 25,000 cycles (Gröbner, 1991a) at bakeout temperature, which is a factor of 100 above the design requirement (Unterlerchner, 1990). This overdesign is believed to be a factor in the high reliability performance of the bellows units. Bellows units are typically tested in special test stands (Rappe, 1982); these are used in the chemical industry for component testing (Rozinskii, 1975). Test stands generally test two bellows units simultaneously so one unit is compressed while the other is expanded. Test stands usually use compressed air (CERN used helium) and electrical heating to achieve the pressure and temperature levels that simulate the working environment. Some 3-5% of all LEP bellows were given the bakeout and ultimate pressure test. The pre-installation testing is used to identify and eliminate weak components ("early life failures") from being mounted on the machine. The description of testing for LEP did not indicate that any batches of bellows were rejected. It is expected that the degree of component testing would depend on the consequences of component failure.

2.2 LEP Bellows Failures

Several authors discussed the bellows units that leaked during the different phases of the LEP project. Gröbner (1991a) stated that 22 standard vacuum bellows leaked upon initial installation, and three standard bellows leaked during initial bakeout sessions. Since the LEP was pre-operational, with only a small operating time under vacuum, these leaks are considered to be weak components or early life failures. The pumpdown time is assumed to be 24 h and the bakeout time is stated to be 24 h, and the installation often performed 2 or 3 such bakeouts (LEP, 1990), so these failure counts and times can be used to calculate an average value of the early life failure rate for the bellows units.

Strubin (1996) discussed the vacuum system and percentages of components that have had vacuum leaks. Five bellows units suffered small vacuum leaks during LEP commissioning and startup in 1989. Gröbner (1992) stated that small leaks at LEP were considered to be on the order of 1E−05 Pa-l/s (1E−08 Pa-m^3/s) throughput leak rate or smaller. As a comparison, the DIII-D tokamak experiment classified vacuum leak rates as follows: a typical throughput leak rate is less than 3E−06 Pa-m^3/s, a small vacuum leak rate is 1E−05 Pa-m^3/s, and a 'stop-and-fix' leak rate is 1E−04 Pa-m^3/s (Cadwallader, 1994). Thus the LEP bellows leaks that occurred were very small leaks by fusion standards. Strubin stated that the LEP bellows leaks were varnished to temporarily seal them. Accelerator experience is that the use of varnish as a leak sealant generally holds fast until a scheduled machine outage allows a maintenance intervention to replace the leaking bellows. However, varnish is not noted to withstand high levels of heating, so this practice probably works best on room temperature components. Gröbner (1990) and Bailey (1992) stated that no bellows failed after machine startup commissioning, so the first year of vacuum operations had no bellows failures. Strubin (1996) also described no additional bellows problems until a bellows leak occurred in 1994, where the throughput leak rate was 1.3E−05 Pa-l/s (1.3E−08 Pa-m^3/s). This was a small leak, and Strubin noted that LEP operations were not delayed by the air leak.

Billy (2000) discussed two separate bellows leaks later in LEP life, and included on a graph that the repair time was on the order of 6.6 hours for both repairs. Thus, the average repair time was 3.3 hours per repair activity. These repairs were not bellows replacement activities since the downtime for venting a sector to replace a bellows unit would be of longer duration (and baking that vacuum sector to restore high vacuum cleanliness would require at least 24 hours). The repairs must have been vacuum leak patching, perhaps identifying the leak location and applying the varnish mentioned earlier. In any case, the repairs were probably temporary to reach a scheduled LEP maintenance outage session. Because the repairs were made in short times, the air leak rates are assumed to be less than 1E−05 Pa-l/s throughput. Therefore, the 3.3 hour average repair time was for locating and temporarily patching a small vacuum leak on a single walled bellows. This time is short and probably not applicable to fusion leak investigation times. Table 2-1 gives the counts of bellows leaks.

Table 2-1. Summary of vacuum bellows leaks in LEP.

Time period	Number of Leaking Bellows	Description	Reference
		Early life time period	
Pre-commissioning	22	Leaks found on initial pumpdown, unknown leak size, assumed to be small	Gröbner 1991a
Pre-commissioning	3	Leaks found on initial bakeout, unknown leak size	Gröbner 1991a
Commissioning (Note: this was 1284 h in 1989)	5	Small leaks	Strubin 1996, Bailey 1992
		Operational life time period	
May 1994	1	Small leak	Strubin 1996
1995–1999	2	Small leaks	Billy 2000

Note: No additional leaks were discussed in any of the LEP final operations documentation available in the literature. Since operational data are not known for the year 2000, the time period for failure rate data calculations will include part of 1989 up to the end of 1999.

2.3 LEP Bellows Operating Times

Several technical papers were found that outlined the LEP operating times. These data are shown in Table 2-2. Particle accelerators tend to be held at vacuum conditions indefinitely, such as for years at a time. Generally, vacuum is only lost to localized vents carried out to perform repairs to the equipment, either internal equipment or the vacuum boundary. The vent times were not found in the literature. However, the accelerator operations are the hours of highest stress to the bellows units, so these are the times considered for LEP operating time. Often, mechanical components, such as engines, hydraulics, etc., have early lifetimes on the order of several weeks to several months (Onwubolu, 2005) and some mechanical and electronic components can have even longer "early lifetimes", even up to a year of operations to reveal fabrication or construction flaws. The LEP bellows units showed weaknesses or flaws

Table 2-2. LEP operating times.

Calendar Year	Annual Scheduled Hours for Physics Operations	Actual Annual Hours of Physics Operations	Reference
1989	1321	469	Bailey 1992
1990	2504	1048	Arduini 1996
1991	2762	1242	Arduini 1996
1992	3439	1742	Arduini 1996
1993	2943	1619	Arduini 1996
1994	3175	1871	Arduini 1996
1995	3070	1414	Arduini 1996
1996		1008	Myers 1997 cited 6 weeks or 1008 hr
1997		1000	Billy 1998
1998		1440	Myers 1999, cited 120 days, assume 50% efficiency
1999		1000	Conservative analyst assumption
Total time		**13,853**	

Notes: The 1999 operating hours were assumed to be equal to the lowest of the recorded annual operations for the matured LEP facility. This assumption for 1999, when beam luminosity had improved greatly over initial operations, is probably an underestimate of the true operating time. This is believed to be a conservative underestimate of 1999 operating hours.
There were no bellows failure data reported for the final year of LEP operation through November 2000; without knowing if any bellows failures occurred in that time period, that year has not been included in this table or in the failure rate calculations.

after much less than a year of operations. From Table 2-1, it is clear that there was an obvious change in failure occurrences from the installation and commissioning time to the first several years of LEP operations. Bailey (1992) pointed out that the commissioning time period was 1,284 hours in 1989. Since no bellows failed after commissioning for several years, the pre-commissioning and the commissioning time appears to be a good indicator of the early life time period of these bellows units.

2.4 Statistical Calculations

The basic component failure rate, the maximum likelihood estimator, is simply λ = (count of failed units)/[(population count)(operating time)] (NRC, 2003). For these bellows units, there are two time periods of interest for which to perform calculations: installation + commissioning (early life failures), and matured lifetime (operational lifetime failures).

Early life failures: From Table 2-1 there were 22 + 3 = 25 failed bellows in pre-commissioning vacuum and bakeout during installation and testing. There were 5 additional bellows that had small leaks in the commissioning, for a total of 30 failed bellows units. Assuming three 48 hour-sessions (a total of 144 hr) of pumping and baking and 1284 hours of commissioning gives

$$\lambda = \text{(30 failures)/[(2649 units)(144 hours+1284 hours)]} \qquad (2\text{-}1)$$

$$\lambda = 7.93\text{E}{-}06\text{/bellows-hour or} \approx 8\text{E}{-}06\text{/bellows-hour} \qquad (2\text{-}2)$$

From NRC (2003) the error bounds for this average failure rate are

5% lower bound failure rate = $\chi^2(2x)/2T$ (2-3)

where

χ^2 = the Chi-square distribution for the 5% tail

x = the number of failures

T = the total population operating time in unit-hours

and

95% upper bound failure rate = $\chi^2(2x+2)/2T$ (2-4)

where

χ^2 = the Chi-square distribution for the 95% tail

and the other variables have been defined above. The values for the Chi-square distribution were taken from a table in O'Connor (1985). The bellows early life failure rate bounds are

- 5% lower bound failure rate = $\chi^2(2x)/2T$, where x = 30 and T = (2649)(1428 hr)
- 5% lower bound failure rate = $\chi^2(60)$/[2(2649)(1428 hr)]
- 5% lower bound failure rate = 43.3/[2(2649)(1428 hr)]
- 5% lower bound failure rate = 5.73E−06/unit-hour or ≈ 6E−06/unit-hour

- 95% upper bound failure rate= $\chi^2(2x+2)/2T$, where x = 30 and T = (2649)(1428 hr)
- 95% upper bound failure rate= χ^2 (62)/2T
- 95% upper bound failure rate= 81.28/[2(2649)(1428 hr)]
- 95% upper bound failure rate= 1.07E−05/unit-hour or ≈ 1E−05/unit-hour

Operational lifetime failures: From Table 2-1, there were a total of 3 bellows small leakage failures over the operational life of the LEP. Several authors commented on these low numbers of faults but verified that these few failures were correct counts for this large population of bellows (Strubin, 1996; Billy, 2000). Table 2-2 gave a total of 13,853 operating hours with beam on for the LEP through 1999. These hours give maximum stress to the bellows and are the time span for the reported bellows failures.

- λ = (3 bellows failures)/[(2649 units)(13,853 hr)]
- λ = 8.18E−08/bellows-hour or ≈ 8E−08/bellows-hour
-
- 5% lower bound failure rate = $\chi^2(2x)/2T$, where x = 3 and T = (2649)(13,853 hr)
- 5% lower bound failure rate = $\chi^2(6)/2T$
- 5% lower bound failure rate = 1.64/[2(2649)(13,853 hr)]
- 5% lower bound failure rate = 2.23E−08/unit-hour or ≈ 2E−08/unit-hour
-

- 95% upper bound failure rate= χ^2 $(2x+2)/2T$, where $x = 3$ and $T = (2649)(13{,}853$ hr)
- 95% upper bound failure rate= $\chi^2(8)/2T$
- 95% upper bound failure rate= 15.5/[2(2649)(13853 hr)]
- 95% upper bound failure rate= 2.11E−07/unit-hour or ≈ 2E−07/unit-hour

These values apply to the failure mode of small vacuum leaks, and small leaks in the LEP had a throughput on the order of 1E−05 Pa-l/s (1E−08 Pa-m^3/s) or less.

There were no reported bellows large leaks or ruptures over the LEP operating time period. A failure rate estimate can be performed to give an indication of the likelihood of such a failure given no occurrences with these bellows units over their operating time. Using a Bayesian approach with a Jeffreys noninformative prior distribution (NRC, 2003) is proper since we have no information about any previous ruptures of this type of bellows used on accelerators. With the Bayesian approach the average failure rate is equal to

$$\lambda = \alpha/\beta \qquad (2\text{-}5)$$

where

α = number of failures counted over the time period + 0.5

β = T+0, the total unit-operating time period + 0 hours.

For the bellows rupture failure mode, there were no failures at LEP and the failure rate calculation is

- λ = (0+0.5)/[(2649)(13,853 h)+0]
- λ = 1.36E−08/unit-hour or ≈ 1E−08/unit-hour

The confidence interval for this "no failures" failure rate can be calculated.

- 5% lower bound failure rate = $\chi^2(2x+1)/2T$, where $x = 0$ and $T = (2649)(13{,}853$ hr)
- 5% lower bound failure rate = $\chi^2(1)/2T$
- 5% lower bound failure rate = (0.00393)/[(2)(2649)(13,853 hr)]
- 5% lower bound failure rate = 5.35E−11/unit-hour or ≈ 5E−11/unit-hour

- 95% upper bound failure rate = $\chi^2(2x + 1)/2T$, where $x = 0$ and $T = (2649)(13{,}853$ hr)
- 95% upper bound failure rate = $\chi^2(1)/2T$
- 95% upper bound failure rate = (3.84)/[(2)(2649)(13,853 hr)]
- 95% upper bound failure rate = 5.23E−08/unit-hour or ≈ 5E−08/unit-hour.

Table 2-3 gives the vacuum bellows failure rates for the different operating periods. While these values are averages, they still serve to show the variation in failure rates from early life to mature component operational life. There is a factor of 100 difference between the early life failure rate and the operational useful life failure rate. The analyst expectation was perhaps a factor of 5 to 10 and certainly < 100, but these are the data results – a somewhat larger number of failures in installation and testing compared to the few failures that occurred in the operating lifetime. The early life value could be influenced by the assumption of a short time interval (144 h) for installation testing of the bellows units. The early life value could also be influenced by the high bakeout temperature during installation tests versus the lower bakeout temperature during the operating lifetime.

Table 2-3. LEP vacuum bellows failure rates.

Time Period	Average Failure Rate in Failures per Bellows-Hour	5% Lower Bound Failure Rate in Failures per Bellows-Hour	95% Upper Bound Failure Rate in Failures per Bellows-Hour
Small vacuum leak failure mode			
Early life (installation and commissioning)	8E−06	6E−06	1E−05
Operational life	8E−08	2E−08	2E−07
Bellows large leak or rupture failure mode			
Operational life	1E−08	5E−11	5E−08
Note: Small vacuum leaks for LEP are on the order of 1E−05 Pa-l/s (1E−08 Pa-m^3/s). Ruptures would have much greater throughput leak rates.			

In comparison, Pinna (2005) cited a vacuum system bellows leakage failure rate from the JET Joint Undertaking of 1.9E−06/bellows-hour. There was not enough information to fully determine the differences between the JET and LEP operational failure rate values, which vary by a factor of 23.75. JET has a smaller population of bellows, so just a few failure events would increase the JET bellows failure rate. If the bellows failure events from external overstress described below in section 2.6 were included in the bellows leakage failure rate, this would explain some of the discrepancy between these two high technology component values. Pinna gave a generic bellows leak value of 4.4E−07/bellows-hour, which is a factor of 5.5 different than the LEP value. For Pinna's generic value it is not known if the bellows population included only vacuum bellows or if other, liquid bellows units were counted as well. Pinna did not state the size of the bellows units. Because of this discrepancy in the LEP and JET failure rate values, a qualitative assessment of LEP value applicability to fusion systems is carried out in the next section.

2.5 LEP Data Applicability to Fusion Systems

The LEP bellows had an operating environment that is close to, but varies somewhat from, the fusion environment. Table 2-4 shows the main differences in a qualitative comparison. Examining the table shows that the operating parameters do not vary greatly, the largest variations being in the accelerator beam (stray GeV particles and creation of nitric acid from beam interactions with humid air outside the accelerator chamber walls) and the accelerator ultrahigh vacuum versus the ITER vacuum exhaust line rough vacuum pressure of ≈2 kPa. These differences are viewed small discrepancies; the ITER bellows would appear to experience a similar or perhaps even a more benign environment than the LEP. The analyst judgment is that the LEP bellows failure rates can be inferred to apply to ITER components. The LEP bellows experience values appear to be more robust than those from JET, but the LEP value comes

Table 2-4. Comparison of LEP and ITER operating environments.

Parameter	LEP Accelerator Vacuum Environment	Expected ITER Regeneration Line Environment
Operating temperature	Expect 15 to 60°C, LEP had beam heatup of 882 W/m, sections had active water cooling	Expect 15-25°C
Temperature excursions	Bakeouts were annual, bellows baked at ≈50°C	Bakeouts could be annual or more frequent, bake at ≈100-200°C
Operating pressure	UHV at 1E−07 Pa	Rough vacuum ≈2 to 3kPa
Pressure excursions	Up to air	Up to air and possibly the expansion of LHe leakage
Mechanical vibration	Very low vibration, < 1 Hz, to prevent magnet jitter (Chao, 1999)	May experience some vibration > 1 Hz
Flow-induced vibration	Expected to be ≈0 in UHV	Perhaps some very low levels of flow vibration in the ITER torus regen line
Mechanical stress	Expected to be low due to low cycles/week	Expected to be low due to low cycles/week
Operating hours/year	Annual hours at vacuum were high, operating availability ≈ 11 to 50%	Annual hours at vacuum should be high, operating availability ≈ 25%
Corrosion	SS used due to possible NHO_3 creation by beam interactions with chamber walls and humid air (Bacher 1990); oxidation	Expect little or no acidic corrosion, oxidation will occur
Flow-induced erosion	Expected to be very low, due to very low pressures and only molecular flow	Expected to be low, due to low pressure and low flow rates
Particle interaction	Bellows were sleeved for RF protection, sleeves offered some protection from stray GeV particles	No GeV particles, perhaps stray MeV particles and keV Beta radiation, no RF energy
Bellows dimensions	0.168 m diameter 0.188 m length	ITER bellows diameters are 0.25 and 0.3 m. Analyst judgment is this is not a driving issue for reliability until the size varies a great deal, i.e., factors of 5 to 10 diameter difference.

from a much larger data set and has not been susceptible to some of the events that JET has suffered. One JET vacuum bellows was overstressed to failure due to forces from radiation shielding movement (ferritic steel plate was inadvertently used as a neutron shield rather than austenitic steel; it moved in the strong magnetic field). Another bellows failed from torque inadvertently applied to it by a diagnostic control system (Wykes, 2010).

2.6 Other Operating Experiences

Orchard (1993) discussed some of the bellows issues at the JET Joint Undertaking. There were two very large leaks resulting from failed bellows. In 1991, a bellows failure resulted in a 2E+06 Pa-l/s leak and in 1992 another bellows failure resulted in a 3E+06 Pa-l/s leak. These two bellows failure events were described above. Both of these leaks caused uncontrolled venting of the vessel and precluded plasma operations. It is interesting to note that Orchard (1993) stated that the time to condition the JET vacuum vessel following a major leak was on the order of seven days: 2 days for bakeout, 4 days for deuterium glow discharge cleaning, and 1 day of helium glow discharge cleaning. Winkel (1990) discussed that JET bellows with high gas or water throughput were prone to excessive vibration and subsequent damage from this flow-induced vibration. Vibration resonances in the bellows could cause cracking failures of individual bellows convolutions even while the entire bellows unit remained within its maximum rated expansion length of travel. Winkel recommended double bellows and interspace pumping, or the use of ventilated, double or triple ply bellows. Presumably 'ventilated' means to draw room air over the bellows unit and capture the sweep air in an air detritiation system. A bellows catalog from a manufacturer stated that standard or typical multi-ply bellows were not recommended for vacuum applications due to possible outgassing into the vacuum system from an undetectable leak in an inner ply (Hyspan, 2002). There are specialized, multi-ply bellows that can be used for vacuum applications, e.g., the Kompaflex 2-ply with woven mesh between plies (see http://www.kompaflex.ch/). The Wendelstein 7-X stellarator is using a multi-ply bellows (Reich, 2007).

Mazzolini (2004) commented that not extending a bellows unit to its rated extension length was found to be a prudent practice for improving bellows lifetime and failure avoidance. This is an application of a design reliability concept referred to as de-rating (Smith, 1997). De-rating means the designer limits the stresses (thermal, mechanical, etc.) on a component to levels below the component's proven capabilities (or rated parameters) to increase the component reliability and lengthen the component service life. De-rating can also provide added protection from anomalies not foreseen in the original design, such as transient loads, electrical surges, etc. (Pecht, 2009).

2.7 Double Bellows

A double confinement design has been suggested for safety because bellows are not as strong as pipe walls. This means a second, independent bellows that is concentric with the primary confinement bellows provides a second confinement barrier. In literature searches, no operating experience data was found that would allow calculation of operational reliability values for dual or concentric bellows. The approach in the ITER Engineering Design Activity (EDA) to address reliability of dual confinement boundaries (such as guard pipes) was to assume that the two sets of components were not completely independent confinement walls since they were in close proximity to each other and could suffer from common effects. There is a possibility of common mode failure for the two concentric bellows units due to common environmental factors such as piping mechanical vibration, impact, and engineering factors of elongation or compression past the rated value, differential thermal expansion, and perhaps other factors. The ITER Safety Analysis Guidelines (Poucet, 1995) suggested a Beta Factor approach to estimate double confinement reliability. At the time of the ITER EDA, the Beta Factor method was one of the leading approaches for modeling common mode failures in Fault Tree Analysis (Andrews, 1993), and it remains a viable approach. The Beta Factor is defined as the ratio of the common cause failure rate to the individual failure rate of a component. The Beta Factor, β, is expressed as a multiplier to the individual component failure rate. Using the multiplier on an individual component failure rate gives the common cause failure rate for any number of multiple component failures. Poucet stated that the Beta Factor for passive equipment should be 0.01 and for active equipment the value should be 0.1. Active equipment requires power (electricity, instrument air, etc.) or a control signal to function. Passive components perform their design function without those requirements and are items such as cables, pipes, tanks, ducts, heat exchangers, bellows, etc. Therefore, to obtain the bellows double confinement failure rate, the best judgment at this time is to multiply the values in Table 2-3 by a passive component factor of 0.01.

The outer bellows would be somewhat larger diameter and create an interspace between the two bellows units. One expansion joint design text suggested that the nominal diameter of the outer bellows be equal to two times the nominal diameter of the inner bellows (Gusenkov, 1996), but this suggestion should be evaluated for ITER. The design idea is to fill the interspace with some gas such as argon, nitrogen, neon, etc., whose unique nature would serve as a telltale marker of leakage into the vacuum system. Orchard (1999) discussed that neon was an attractive choice as an interspace gas since it has the virtues of no long-lived neutron activation products, it has little or no effect on machine conditioning, and neon has a specific mass spectra footprint at mass 22 that is easily detected amid carbon-hydrogenic compounds in tokamaks. Orchard suggested an initial interspace pressure of 500 mbar (50 kPa), and that the pressure be monitored. A neon pressure increase would indicate a room air leak into the interspace and a neon pressure decrease would indicate an interspace gas leak through the primary barrier into the vacuum piping. Monitoring would be by way of a port in the bellows flange rather than a penetration of the bellows wall.

2.8 Conclusions

The LEP operated a large number of bellows and published sufficient information to allow calculation of single-walled, stainless steel vacuum bellows failure rate values for small vacuum leaks. Using statistics, a bellows failure rate for large leaks or ruptures was also calculated based on no failures of that type occurring at the LEP over its operating lifetime. The bellows failure rates found here and given in Table 2-3 are believed to be applicable to similar types of ITER vacuum bellows (i.e., circular, stainless steel bellows units). The ITER EDA approach for dual confinement has been applied to these stainless steel bellows failure rates to obtain leakage values for double confinement bellows, as given in Table 2-5. Some design ideas have been mentioned for consideration in ITER bellows design, including an inert gas filled, pressure-monitored interspace, and de-rating the bellows to improve longevity.

Table 2-5. Suggested ITER double confinement vacuum bellows failure rates.

Time Period	Average Failure Rate in Failures per Double Bellows-Hour	5% Lower Bound Failure Rate in Failures per Double Bellows-Hour	95% Upper Bound Failure Rate in Failures per Double Bellows-Hour
Small vacuum leak failure mode			
Operational life	8E−10	2E−10	2E−09
Bellows large leak or rupture failure mode			
Operational life	1E−10	5E−13	5E−10

2.9 References

Andrews, 1993. J. D. Andrews and T. R. Moss, Reliability and Risk Assessment, Longman Scientific & Technical, Essex, UK (1993) 206-208.

Arduini, 1996. G. Arduini, R. Bailey, T. Bohl, F. Bordry, H. Burkhardt, K. Cornelis, P. Collier, A. Faugier, V. Hatton, M. Jonker, M. Lamont, J. Miles, G. de Rijk, G. Roy, H. Schmickler, J. Wenninger, "LEP1 Operation, 1989-1995," Proceedings of the Fifth European Particle Accelerator Conference (EPAC-96), Sitges (Barcelona), Spain, June 10-14, 1996, Taylor & Francis, London (1996) 286-288.

Bacher, 1990. J. P. Bacher and N. Hilleret, "Corrosion of accelerator vacuum systems: risks and prevention," Vacuum, 41 (1990) 1914-1916.

Bailey, 1990. R. Bailey, T. Bohl, F. Bordry, P. Collier, K. Cornelis, B. Desforges, A. Faugier, V. Hatton, H. Laeger, J. Miles, J. Poole, G. de Rijk, H. Schmickler, D. Vandeplassche, "First Operational Experiences with LEP," Proceedings of the Second European Particle Accelerator Conference (EPAC 90), Nice, France, June 12-16, 1990, Editions Frontieres, Cedex, France (1990) 401-402.

Bailey, 1992. R. Bailey, T. Bohl, F. Bordry, H. Burkhardt, K. Cornelis, P. Collier, B. Desforges, A. Faugier, V. Hatton, M. Lamont, J. Miles, G. de Rijk, H. Schmickler, "Three Years Operational Experience with LEP," Proceedings of the Third European Particle Accelerator Conference (EPAC 92), Berlin, Germany, March 24-28, 1992, Editions Frontieres, Cedex, France (1992) 63-65.

Bailey, 1993. R. Bailey, T. Bohl, F. Bordry, H. Burkhardt, K. Cornelis, P. Collier, B. Desforges, A. Faugier, V. Hatton, M. Jonker, M. Lamont, J. Miles, G. de Rijk, H. Schmickler, "LEP Operation in 1992 with a 90° optics," Proceedings of the 15th Particle Accelerator Conference (PAC 93), Washington, DC, May 17-20, 1993, IEEE (1993) 2001-2003.

Billy, 1998. J. C. Billy, J. P. Bojon, N. Hilleret, M. Jimenez, I. Laugier, "Experience with the LEP Vacuum System at Energies Above 90 GeV and Future Expectations," Proceedings of the Sixth European Particle Accelerator Conference, (EPAC 98), Stockholm, Sweden, June 22-26, 1998, Taylor & Francis, London (1998) 314-316.

Billy, 2000. J. C. Billy, J. P. Bojon, O. Gröbner, N. Hilleret, M. Jimenez, I. Laugier, P. Strubin, "The LEP vacuum system: a summary of 10 years of successful operation," Proceedings of the Seventh European Particle Accelerator Conference (EPAC 2000), Vienna, Austria, June 26-30, 2000, 2286-2288.

Bryan, 2009. S. Bryan, ITER International Organization, vacuum group, private communication, September 30, 2009.

Cadwallader, 1994. L. C. Cadwallader, Vacuum System Operating Experience Review for Fusion Applications, EGG-FSP-11037, Idaho National Engineering Laboratory, March 1994.

Chao, 1999. A. Wu Chao, M. Tigner, Handbook of Accelerator Physics and Engineering, World Scientific Press, Singapore (1999) chapter 5.

Gröbner, 1990. O. Gröbner, “The Performance of the Ultra-High Vacuum System of the LEP and the Experience Gained During the First Year of Operation,” Proceedings of the Second European Particle Accelerator Conference (EPAC 90), Nice, France, June 12-16, 1990, Editions Frontieres, Cedex, France (1990) 337-339.

Gröbner, 1991. O. Gröbner, “General considerations in the design of accelerator vacuum systems,” Journal of Vacuum Science and Technology, A9 (1991) 2074-2080.

Gröbner, 1991a. O. Gröbner, P. M. Strubin, “LEP Vacuum System Start-Up and Operation Experience,” American Institute of Physics Proceedings, 236 (1991) 18-29.

Gröbner, 1992. O. Gröbner, “The design and performance of the LEP vacuum system at CERN,” Vacuum, 43 (1992) 27-30.

Gusenkov, 1996. A. P. Gusenkov, B. Yu. Lukin, V. S. Shustov, Standardization and Design Optimization of Flexible Piping Elements, Begell House, Inc., publishers, Redding, Connecticut, USA (1996) p. 59.

Hyspan, 2002. Series 7500, Formed Metal Bellows, Catalog 974C, Hyspan Precision Products, Inc., Chula Vista, California, catalog available at www.hyspan.com.

Lamont, 2001. M. Lamont, R. Assman, and B. Goddard, “Lessons Learned from LEP,” Proceedings of the 2001 Particle Accelerator Conference, Chicago, IL, June 18-21, 2001, IEEE (2001) 3502-3504.

LEP, 1984. LEP Design Report, Volume II, The LEP Main Ring, CERN-LEP/84-01, European Organization for Nuclear Research, June 1984, section 8.4.9.

LEP, 1985. Specification for the Standard Bellows Assemblies of the LEP Main-Ring Vacuum System, I-1318/LEP. LEP-VA/WU/sm, European Organization for Nuclear Research, February 1985.

LEP, 1990. LEP Vacuum Group, “LEP vacuum system: present status,” Vacuum, 41 (1990) 1886-1990.

Mazzolini, 2004. F. Mazzolini, L. Rumiz, J. Miertusova, F. Pradal, “Ten Years of ELETTRA vacuum experience,” Vacuum, 73 (2004) 225-229.

Myers, 1997. S. Myers, “LEP2: Present and Future Performance and Limitations,” Proceedings of the 17th Particle Accelerator Conference (PAC97), Vancouver, Canada, May 12-16, 1997, IEEE (1997) 1-5.

Myers, 1999. S. Myers, “High Energy Operation of LEP2,” Proceedings of the Particle Accelerator Conference, (PAC-99),” New York, New York, March 29-April 2, 1999, IEEE (1999) 299-303.

NRC, 2003. C. L. Atwood, J. L. LaChance, H. F. Martz, D. J. Anderson, M. Englehardt, D. Whitehead, T. Wheeler, Handbook of Parameter Estimation for Probabilistic Risk Assessment, NUREG/CR-6823, US Nuclear Regulatory Commission, Washington, DC (September 2003) page 6-6.

O’Connor, 1985. P. D. T. O’Connor, Practical Reliability Engineering, second edition, John Wiley & Sons, Publishers, New York (1985) appendix 3.

O'Hanlon, 2003. J. F. O'Hanlon, A User's Guide to Vacuum Technology, third edition, John Wiley & Sons, Inc., Somerset, NJ (2003) section 17.2.

Onwubolu, 2005. G. C. Onwubolu, Mechatronics: principles and applications, Butterworth-Heinemann, London (2005) page 568.

Orchard, 1993. J. C. Orchard, A. T. Peacock, and G. Saibene, "JET experience in recovery from large air leak incidents," Journal of Nuclear Materials, 200 (1993) 395-399.

Orchard, 1999. J. C. Orchard, S. C. Scales, "The JET vacuum interspace system," Vacuum, 53 (1999) 357-361.

Pecht, 2009. M. G. Pecht, editor, Product Reliability, Maintainability and Supportability Handbook, second edition, CRC Press, Boca Raton, Florida (2009) 208.

Pinna, 2005. T. Pinna, G. Cambi, S. Ciattaglia, A. Lo Bue, S. Knipe, J. Orchard, R. Pearce, U. Besserer, "Collection and analysis of data related to fusion machines (JET and TLK) operating experience on component failure," Fusion Engineering and Design, 75-79 (2005) 1199-1203.

Poucet, 1995. A. E. Poucet et al., Safety Analysis Guidelines, version 1, ITER Joint Central Team, S 81 RI 1 95-12-13 F1, San Diego Joint Work Site (December 1995).

Rappe, 1982. G. H. Rappe, G. Brown, E. D. Perry, "Fatigue Testing of TFTR Vacuum Bellows," Proceedings of the 9th Symposium on Engineering Problems of Fusion Research, Chicago, Illinois, October 26-29, 1981, IEEE (1982) 240-243.

Reich, 2007. J. Reich, A. Cardella, A. Capriccioli, T. Koppe, B. Missal, W. Löhrer, S. Langone, P.-C. Sassone, "Experimental verification of the axial and lateral stiffness of large W7-X rectangular bellows," Fusion Engineering and Design, 82 (2007) 1924-1928.

Rozinskii, 1975. I. N. Rozinskii, G. M. Zakharova, and E. Kh. Burdo, "Stand for Testing Bellows," Chemical and Petroleum Engineering, 11 (1975) 578-579.

Smith, 1997. D. J. Smith, Reliability, Maintainability and Risk, fifth edition, Butterworth-Heinemann, London (1997) chapter 10.

Strubin, 1996. P. M. Strubin, J.-P. Bojon, "Reliability of the LEP Vacuum System: Experience and Analysis," Proceedings of the 16th IEEE Particle Accelerator Conference, Dallas, Texas, May 1-5, 1995, IEEE (1996) 2014-2016.

Unterlerchner, 1990. W. Unterlerchner, "Non-standard vacuum hardware for an accelerator vacuum system," Vacuum, 41 (1990) 1920-1923.

Winkel, 1990. T. Winkel, J. Orchard, "Leak evaluation in JET and its consequences for future fusion machines," Vacuum, 41 (1990) 1988-1991.

Wykes, 2010. M. E. P. Wykes, ITER consultant, private communication, January 8, 2010.

3. PRELIMINARY FAILURE RATE ESTIMATES FOR ELECTRICAL INSULATING BREAKS IN ITER CRYOGENIC SYSTEMS

In late February 2010, Mr. Craig Hamlyn-Harris of the ITER International Organization (IO) Vessel Division requested failure rate data for cryogenic components, including the electrical insulators used in pipe sections as electrical isolation of the pipe run against magnetic field-induced electrical current in the pipe walls.

3.1 Approach to Estimate Failure Rates

The best approach for estimating reliability of components is to determine the reliability of the same type of component that is operating in the same, or similar, environment. Therefore, the component performance at existing fusion experiments was reviewed to determine the operating experiences of these electrical insulating breaks. It is believed that nearly all particle accelerators and magnetic fusion experiments use these units to prevent stray electrical current flow in the pipe walls, but it was determined from a literature search that discussion of their reliability has not been published in any detail. This lack of discussion suggests that the components are not failing since discussions tend to focus on the components whose failures create downtime and personnel safety concerns. Nonetheless, Yoshida (1996) pointed out in the ITER EDA that the ceramic breaks were considered to be weak components compared to the metal piping, and the breaks could leak. The locations of the ceramic breaks had to be chosen with care since they could fail during the life of the ITER facility and therefore the ceramic breaks required the ability to be replaced by hands-on maintenance. Taking Yoshida's speculation on a ceramic break failure in 20 years would give a failure rate of 1 failure/(1 unit)(20 y)(8760 hr/yr), or a gross failure rate estimate value of 5.7E−06/hour-unit, which would be a good failure rate for active equipment but is a rather high failure rate for most passive equipment that is part of a pipe pressure boundary.

There are three pieces of data needed to estimate a failure rate. These are the count of failure events involving the components under study at the facility, the count of components in the facility, and the operating time of the components. As a generality, most failure events are discussed in the literature, but the component population is not. The facility operating time may or may not be discussed.

It was noted that the US Department of Energy (DOE) fusion safety design guidance discusses ceramic breaks. The DOE guidance is in two parts. First, the use of ceramic breaks should be minimized, and when these components are used, they should be qualified by analysis or testing in the anticipated operating and design basis off-normal event environment to demonstrate the required confinement integrity (DOE, 1996). That guidance is in agreement with Yoshida's concerns stated above. Second, the guidance discussed positioning ceramic breaks out of direct line-of-sight with the plasma to minimize heating and radiation damage. Redundant ceramic breaks were recommended for use in the radiofrequency plasma heating lines since a failure in a single ceramic break unit was believed to result in a loss of vacuum event for the vacuum vessel (DOE, 1999).

3.2 Literature Review of Operating Experiences

Scientific facilities using large cryoplants were examined to determine if there were any operating experiences with ceramic insulator breaks in cryogenic piping. The ITER environment is flowing, gaseous helium at 80 K and 1.8 MPa; however, given the sparsity of published operating experiences any ceramic break data would be useful.

The Tore Supra fusion experiment has a cryoplant sized to cool a set of superconducting toroidal field magnets (Claudet, 1986), and this fusion machine is a preferred source to collect operating experience data from its many published operating experiences. Insulated breaks have been used on Tore Supra (Bon Mardion, 1992) in stainless steel 304L cryogenic pipe. The breaks are fabricated from fiberglass insulation rather than alumina. The bonding method was not mentioned in the description of these units. There are ten 'insulating break' units, with internal and external diameters given in Figure 3-1. In this case, the component is similar to the envisioned alumina insulator, and in the same application as the ITER units.

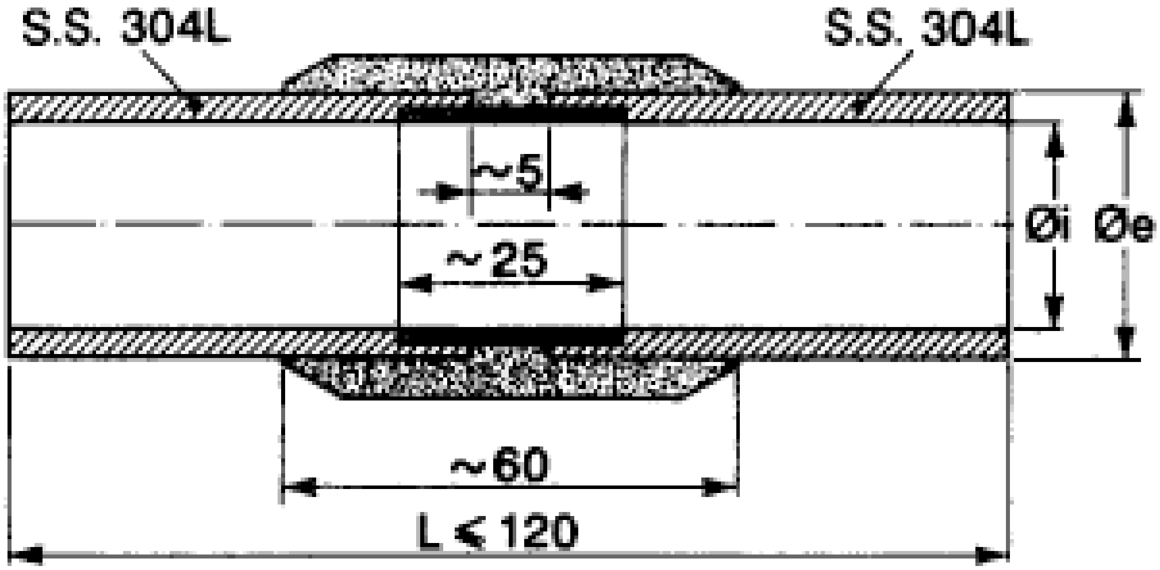

items	number	Øi (mm)	Øe (mm)
1	1	100	104
2	8	39.2	42.4
3	1	10	12

Figure 3-1. Sketch of a Tore Supra insulated break, helium tight, < 1,000 volts.
Note: This figure was taken from Bon Mardion, 1992.

Mr. Hamlyn-Harris spoke with Dr. Jean-Luc Duchateau and Dr. Pascal Reynaud of the Tore Supra cryogenic department on March 12, 2010. The operating experience information discussed was that two of the insulating breaks failed during initial system commissioning in the 1986 time frame. These units were replaced. The failure mechanism was not discussed, but the units leaked only at cryogenic temperature and not at room temperature. It is not certain, but suspected, that improper flange bolt torquing was involved; this can lead to leakage when flanges are cooled down to cryogenic temperature but is not apparent at room temperature. Replacing the units would allow renewal of the flange seal surfaces and provide an opportunity for rebolting the flanges. Since 1987, the insulating breaks in the Tore Supra cryogenic system have performed without failure. Thus, from the first time that the cryogenic system was in full operation to cool down the Tore Supra magnet set in early 1988, the insulating breaks in the cryolines have operated without failure. An engineering assumption is made that the two units that failed during system commissioning are identified as 'early life' failures and that the probable failure mechanism would not be expected to occur during the operating life of the cryogenic system because the insulating breaks are not being opened or replaced if they are not faulty. Therefore, the failure rate will be calculated based on no observed failures of the insulating breaks over the 1988-2010 time frame.

Tore Supra has published the highlights of engineering operations data on its cryoplant. Libyere (2005) stated that a typical year for the Tore Supra cryogenic system is 9 months of continuous operation, monitored by an automatic control system and a staff of 12 people.

Other literature reviewed for this task also shows no events of insulating break leakage or other failure have occurred at Tore Supra (Bon Mardion, 1988; Bon Mardion, 1990; Gravil, 1991; Claudet, 1993; Gravil, 1994; Gravil, 1996; Turck, 1996; Minot, 1997; Gravil, 1998; Gravil, 1998a). Minot (1997) mentioned that the Tore Supra cryogenic system as a whole typically leaks 2E−04 m^3/second (200 cc/s) of gaseous helium, mainly from the compressor section, and that leakage is not attributed to faults in the insulating breaks.

Obert (1996) reported that the Joint European Torus (JET) tokamak cryolines with insulating breaks did not require any remedial work or maintenance in the time from 1983 to 1996. Therefore, the assumption that these components can be reliable would appear to be a reasonable assumption since 50 of these units have operated at a high duty factor, 50 to 75% operating time per year (Obert, 1994), for more than a decade without any failures. This experience can be added to the Tore Supra experience: the JET count of 50 insulating breaks, no failures, over 13 years at a conservatively low assumption of 50% operations (or 180 days) per year in that time period.

3.3 Insulating Break Failure Rate Calculation

The Tore Supra operating experience data indicate that there were no insulating break failures over the ≈22 years of Tore Supra operations from 1988 through the beginning of 2010, with ten insulating break units operating in that time period. From Obert's JET data, 50 insulating breaks have been used and none failed over a known 13-year period. The US Nuclear Regulatory Commission approach to failure rate estimation with no failure events (Atwood, 2003) is λ=0.5/T, where T is the total operating time for all of the units. A reasonable assumption is that all insulating break units operate when the cryoplant operates. Libyere (2005) stated that the Tore Supra cryoplant has 9 months continuous operation per calendar year, that is ≈270 days/year. Gravil (1994, 1998a) stated that in the first seven and ten years of cryogenic plant operation, the system had accumulated over 45,000 and 65,000 hours, respectively – which agrees with Libyere's estimate of 75% operations in a year. Also, on March 12, 2010, the Tore Supra staff confirmed to Mr. Hamlyn-Harris that the cryogenic system has been operating with the "9 months on and 3 months off" schedule consistently. The JET cryoplant plant was assumed to have 180 days of operation each year and 50 insulating break units with no failures. Therefore, for the combined experiences of the Tore Supra and JET insulating break units, the total T=(10 units)(22 years)(270 days/year)(24 hr/day) + (50 units)(13 years)(180 days/year)(24 hr/day) or 4.234E+06 unit-hours of operation. The average failure rate for zero events would be λavg=0.5/4.234E+06 unit-hours, or 1.2E−07/unit-hour. Rounding off is prudent due to the assumptions about operating time, giving a failure rate of 1E−07/unit-hour. An upper bound failure rate (Atwood, 2003) with a 95% Chi-square distribution and 2n+2 degrees of freedom (where n=number of failure events) is χ2(0.95,2)/2T. The χ2(0.95,2)=5.99 as found from Chi-square tables in O'Connor (1985). The upper bound failure rate calculation is

(5.99)/(2)(4.234E+06 unit-h) or 7.1E−07/unit-hour. Rounding off this value would give 7E−07/unit-hour. The Chi-square 5% lower bound failure rate calculation with 2n+1 degrees of freedom would be (0.103)/(2)(1.426E+06 unit-h), or 1.2E−08/unit-hour. Rounding off this value would give 1E−08/unit-h. This insulating break failure rate is a coarse value, and it is a 'general' failure rate since no specific failure has occurred to identify a mode of failure. This rate would be applied to any individual failure mode (e.g., leaks, ruptures, clogging) until some event data accumulate to identify the modes of failure. It is recognized that different component failure modes have different failure rates, but for the present time, this single value for any failure mode will have to suffice until more detailed information becomes available:

- Insulating break average failure rate (any failure mode) 1E−07/hour
- Insulating break 95% upper bound failure rate (any failure mode) 7E−07/hour
- Insulating break 5% lower bound failure rate (any failure mode) 1E−08/hour

3.4 Friction Joint Leakage Failure Rate Calculation

In the course of Mr. Hamlyn-Harris' investigation on March 12, 2010, the Tore Supra staff told him that there had been one leak on an aluminum-to-stainless steel (Al-SS) friction joint on the 4 K cryogenic lines. A friction joint is fabricated by rotating one pipe at a high speed and driving it to enter the end of a second pipe. The friction heat melts the metals, and when cooled they form a welded joint. There are 130 of these Al-SS friction joints in the Tore Supra cryogenic system. Therefore, the mean failure rate calculation would be λ_{avg}=n/T (Atwood, 2003) where n is the number of failures of this particular unit and T is the total operating time of all units. The operating time was estimated in the previous section. In this case, n=1 leakage failure and T=(130 units)(22 years)(270 days per year)(24 hr/day) or 1.85E+07 unit-hours. The leakage was not described well and it is assumed to be a small leakage event (e.g., a leak rate perhaps on the order of 1 cm^3/s) rather than a large leak or rupture event. The friction joint leakage failure rate is λ_{avg} = 1 leak/1.85E+07 unit-hours, or 5.4E−08 per unit-hour which rounds off to 5E−08/hr. The 95% Chi-square upper bound would be based on 2n+2 degrees of freedom and the 5% Chi-square lower bound would be based on 2n degrees of freedom. $\lambda_{95\%} = \chi^2(0.95,4)/2T$, or $\lambda_{95\%}$ = 9.49/[2(1.85E+07 unit-h)]. $\lambda_{95\%}$ = 2.56E−07/unit-hour, which rounds off to 3E−07/hr for one unit. The lower bound failure rate calculation is $\lambda_{5\%} = \chi^2(0.95,2)/2T$, or $\lambda_{5\%}$ = 0.103/[2(1.85E+07)]. $\lambda_{5\%}$ = 2.8E−09/unit-hour, which rounds off to 3E−09/hr for one unit.

- Friction joint average failure rate (leakage failure mode) 5E−08/hour
- Friction joint 95% upper bound failure rate (leakage failure mode) 3E−07/hour
- Friction joint 5% lower bound failure rate (leakage failure mode) 3E−09/hour

3.5 Conclusions

Table 3-1 gives the failure rate estimates for the Tore Supra and JET cryogenic insulating breaks and Tore Supra cryogenic friction joints. These failure rates are calculated from rough data based on overall operating experiences from tokamaks. Tokamaks are viewed as the best data source for operating experiences applicable to ITER components. However, no tokamak operating records were examined for either Tore Supra or JET, especially the operating times, so these failure rate values are considered to be coarse estimates. These coarse values should reflect the order of magnitude of obtainable failure rates for the insulating breaks and the friction joints, and these values should suffice for initial reliability studies. It is anticipated that at some point in the future a component vendor will be selected to provide components to ITER and the selected vendor could, under contract, share their detailed reliability data with ITER designers.

Table 3-1. Cryogenic component failure rate estimates.

Component and Failure Mode	Average Failure Rate in Failures per Hour	5% Lower Bound Failure Rate in Failures per Hour	95% Upper Bound Failure Rate in Failures per Hour
Insulating break, any failure mode	1E−07	1E−08	7E−07
Al-SS friction joint, small leakage failure mode	5E−08	3E−09	3E−07

3.6 References

Atwood, 2003. C.L. Atwood, J.L. LaChance, H.F. Martz, D.J. Anderson, M. Englehardt, D. Whitehead, T. Wheeler, Handbook of Parameter Estimation for Probabilistic Risk Assessment, NUREG/CR-6823, Nuclear Regulatory Commission, Washington, DC, September (2003), chapter 6.

Bon Mardion, 1988. G. Bon Mardion, G. Claudet, G. Ferlin, B. Gravil, B. Jager, L. Tavian, "Initial Operation of the 1.8 K Tore Supra Cryogenic System," Proceedings of the Twelfth International Cryogenic Engineering Conference (ICEC 12), Southampton, UK, July 12-15, 1988, Butterworth & Co., Surrey, UK (1988) 511-518.

Bon Mardion, 1990. G. Bon Mardion, G. Ferlin, B. Gravil, B. Jager, L. Tavian, "Normal operation of the 1.8 K Tore Supra Cryogenic System," Cryogenics, 30S (1990) September Supplement for ICEC-13, 566-570.

Bon Mardion, 1992. G. Bon Mardion, B. Gravil, B. Jager, "The Tore Supra, Flexible and Electrically Insulating, Cryogenic Connection Line," Cryogenics, 32, ICEC Supplement (1992) 142-145.

Claudet, 1986. G. Claudet, G. Bon Mardion, B. Jager, and G. Gistau, "Design of the cryogenic system for the Tore Supra tokamak," Cryogenics, 26 (1986) 443-449.

Claudet, 1993. G. Claudet, "The Tore Supra He II cryogenic system," Fusion Engineering and Design, 20 (1993) 485-490.

DOE, 1996. Safety of Magnetic Fusion Facilities: Guidance, DOE-STD-6003-96, US Department of Energy, Washington, DC, May 1996, page 89.

DOE, 1999. Supplementary Guidance and Design Experience for the Fusion Safety Standards DOE-STD-6002-96 and DOE-STD-6003-96, DOE-HDBK-6004-99, US Department of Energy, Washington, DC, January 1999, page 10.

Gravil, 1991. B. Gravil, B. Bon Mardion, G. Ferlin, B. Jager, L. Tavian, "Two Years of Operation of the Tore Supra Cryogenic System," Fusion Technology 1990, Proceedings of the 16th Symposium on Fusion Technology, London, UK, September 3-7, 1990, North-Holland, Amsterdam (1991) 1649-1653.

Gravil, 1994. B. Gravil, G. Bon Mardion, B. Jager, F. Minot, "Back-up Systems of the Tore Supra Superconducting Toroidal Magnet Refrigeration," Cryogenics, 34 (1994) 69-72.

Gravil, 1996. B. Gravil, B. Jager, F. Minot, “10 Years of Operation of the Tore Supra Cryogenic System,” Proceedings of the Symposium on Cryogenic Systems for Large Scale Superconducting Applications, May 27-29, 1996, Toki, Japan, report NIFS-PROC-28 (1996) 8-11. Available at: www.nifs.ac.jp/report/NIFS-PROC-028.pdf.

Gravil, 1998. B. Gravil, D. Henry, F. Minot, and the Tore Supra cryogenic team, “Operation with the 1.8 K Tore Supra Cryogenic System,” Fusion Technology, 34 (1998) 680-683.

Gravil, 1998a. B. Gravil, B. Jager, “Experience with a Large Scale He II Refrigeration System at Tore Supra, P. Kittel, editor, Advances in Cryogenic Engineering, 43, Proceedings of the 1997 Cryogenic Engineering Conference, Portland, Oregon, Plenum Press (1998) pages 571-579.

Libyere, 2005. P. Libyere, J. L. Duchateau, B. Gravil, E. Tena, D. Henry, J. Y. Journeaux, “Pioneering superconducting magnets in large tokamaks: Evaluation after 16 years of operating experience in Tore Supra,” Fusion Engineering and Design, 75-79 (2005) 221-228.

Minot, 1997. F. Minot, G. Bon Mardion, B. Jager, B. Gravil, J. L. Marechal, J. L. Violet, “A New Concept to Detect He Leaks on Tore Supra Cryogenic Plant,” Proceedings of the 16th International Cryogenic Engineering Conference (ICEC-16), Kitakyushu, Japan, May 20-24, 1996, Elsevier, 1997, 689-692.

Obert, 1994. W. Obert, “The JET Cryosystem, Overview and Experience,” in P. Kittel, editor, Advances in Cryogenic Engineering, 39, Proceedings of the 1993 Cryogenic Engineering Conference, Albuquerque, New Mexico, July 12-16, 1993, Plenum Press (1994) pages 493-500.

Obert, 1996. W. Obert, “JET experience with the large scale cryogenic system,” Proceedings of the Symposium on Cryogenic Systems for Large Scale Superconducting Applications, May 27-29, 1996, Toki, Japan, report NIFS-PROC-28 (1996) 16-19. Available at: www.nifs.ac.jp/report/NIFS-PROC-028.pdf.

O’Connor, 1985. P. D. T. O’Connor, Practical Reliability Engineering, second edition, John Wiley & Sons, Inc., Chichester, 1985, pages 353-354.

Turck, 1996. B. Turck, “Six years of operating experience with Tore Supra, the largest Tokamak with superconducting coils,” IEEE Transactions on Magnetics, 32 (1996) 2264-2267.

Yoshida, 1996. K. Yoshida, V. Kalinin, S. Stoner, T. Kato, “Requirements and interfaces to cryogenic and power supply plants for the ITER magnet system,” in P. Kittel, editor, Advances in Cryogenic Engineering, 41, Proceedings of the 1995 Cryogenic Engineering Conference, July 17-21, 1995, Columbus, Ohio, Plenum Press (1996) pages 701-708.

4. FAILURE RATE ESTIMATE FOR STAINLESS STEEL PIPING USED IN THE ITER VACUUM SYSTEM

The designers in the ITER Vacuum Group have reviewed the safety direction of using double walled pipe with monitored interspace to negate the possibility of room air inleakage to vacuum piping. The safety concern is that inleakage air mingling with the hydrogen species (H, D, or T) released during cryopump regeneration could present sufficient conditions to result in a hydrogen explosion. To address this safety concern, the designers have chosen to use double containment of all the 'weak' components used in the regeneration and forelines, including instrumentation feedthroughs, circular bellows for pipe expansion and contraction, valve stems, etc. The piping has been tentatively selected to be single-walled stainless steel 304, schedule 20. The SS regeneration pipe runs for approximately 160 m length. This document gives the leakage failure rate for this type of piping to show that the failure rate is appropriately low.

4.1 Preliminary Description of the Vacuum Piping

The ITER cryopump regeneration line will be 300 mm diameter, single walled pipe, as shown in Figure 4-1. Typical vacuum piping tends to be thin-walled since the pressure difference is only 1 atmosphere, which is not a high pressure for metal pipe. A typical vacuum supply company's web-based catalog (e.g., www.lesker.com) gives 3.175 mm (0.125-inch) wall thickness for 304.8 mm-diameter SS vacuum tubing. This tubing wall thickness is less than schedule 5 for DN 300 mm stainless steel pipe; schedule 5 pipe is 3.96 mm and schedule 10 is 4.57 mm wall thickness (ASME, 2004). Table 4-1 gives pipe schedules. The ITER piping will be constructed of SS304, presumably Unified Numbering System (UNS) S30400, or SS304L, UNS S30403. Stainless steel was chosen for superior corrosion resistance to the gaseous products released from the cryopumps, including organic molecules, water vapor, and air. Stainless steel also has the benefits of fabricability, versatility in applications, and economy (that is, due to its popularity the costs of stainless steel are moderate). The piping wall thickness was tentatively selected to be schedule 20, or 6.3 mm wall thickness to add robustness to the pipe. Schedule 20 is more than twice the thickness of the typical vacuum tubing, although schedule 10 pipe is also under consideration. The piping will be welded by single pass tungsten inert gas (TIG) welding; an advantage of schedule 20 or less wall thickness is that the weld requires only a single pass rather than multiple passes. The single pass weld is regarded by the designers to be inherently more reliable than multi-pass welds. Presumably this is due to fewer weld flaws and inclusions in the single-pass welds than multi-pass welds. Single pass, continuous welds are also beneficial to reduce virtual leaks in the vacuum system. There will be 100% weld radiography on fabrication and full leak testing of completed lines. The regeneration piping is part of the ITER vacuum vessel confinement boundary, so the pipe will be protected against seismic events with the ITER machine seismic isolation pads, plus appropriate pipe hangers, pipe supports, and/or snubbers as needed to guarantee that piping remains intact in the safe shutdown earthquake event. Seismic protection includes examination of the effects of pipe oscillation, pipe whip and impacts from adjacent pipes or equipment during a seismic event. The piping will use circular, hydroformed convolution bellows to accommodate thermal expansion and contraction of the pipe. As mentioned, the bellows will be double walled or double ply, and they will be protected from seismic events similar to the lengths of pipe, using either tie rods, supports, or guides to restrict pipe motion on either side of the bellows units.

ISOMETRIC VIEW OF TORUS CRYOPUMP REGENERATION FORELINE AND CRYOSTAT FORELINE

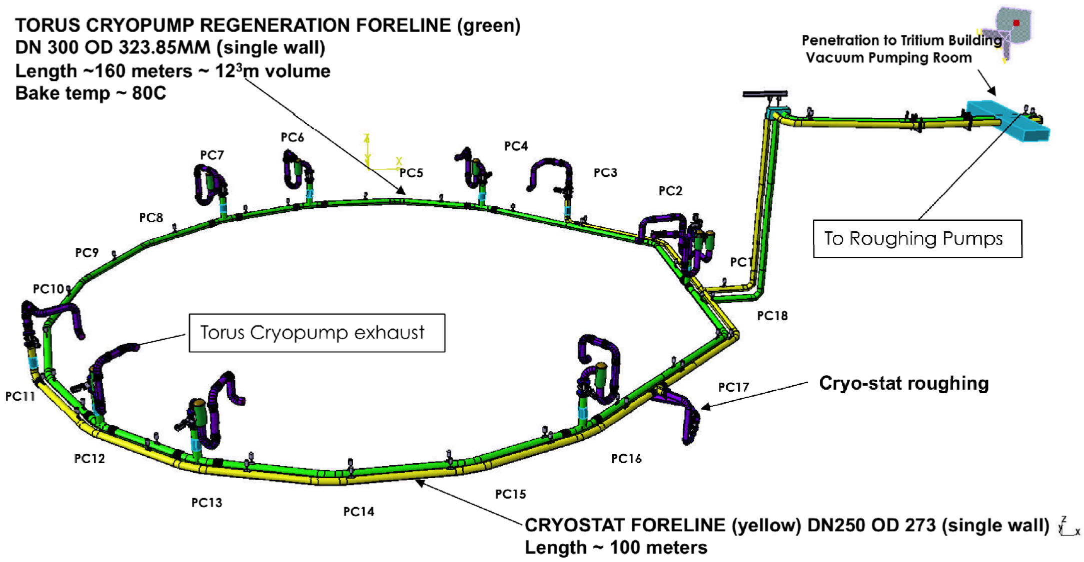

Figure 4-1. The ITER regeneration and cryostat forelines.

4.2 ITER Vacuum Pipe Service Environment

The stainless steel regeneration piping will operate whenever there is cryopump regeneration. The operational plan is to regenerate cryopumps individually and sequentially during ITER operations. Each cryopump will have staged regeneration during plasma operations. The first stage is to remove elemental gases, so there is flow of helium and protium hydrogen species during cryopump regeneration that takes place during plasma operations. Day (2006) gave the typical fusion exhaust gas compositions for ITER, which are

Constituent	mol%
Protium and helium	6.5
Deuterium and tritium	78.5
Air-likes and inert gases (non-tritiated)	11.0
Organic molecules (tritiated)	3.3
Water vapor (tritiated)	0.7

Table 4-1. Dimensions of steel piping in SI units.

DN	Pipe Schedule	Identifier	Outside Diameter (mm)	Wall Thickness (mm)	Plain End Pipe Mass (kg/m)
			Carbon steel piping		
150	40	STD	168.3	7.11	28.26
	80	XS	168.3	10.97	42.56
	160	XXS	168.3	21.95	79.22
200	40	STD	219.1	8.18	42.55
	80	XS	219.1	12.70	64.64
	160	XXS	219.1	23.01	111.27
300	40	STD	323.8	10.31	79.71
	80	XS	323.8	17.48	85.82
	120	XXS	323.8	25.40	186.92
350	30	STD	355.6	9.53	81.33
	40	XS	355.6	12.70	107.40
			Stainless steel piping		
150	5S		168.3	2.77	11.31
	10S		168.3	3.40	13.83
	40S		168.3	7.11	28.26
	80S		168.3	10.97	42.56
200	5S		219.1	2.77	14.78
	10S		219.1	3.76	19.97
	40S		219.1	8.18	42.55
	80S		219.1	12.70	64.64
250	5S		273.1	3.40	22.61
	10S		273.1	4.19	27.79
	40S		273.1	9.27	60.31
	80S		273.1	12.70	81.56
300	5S		323.9	3.96	31.25
	10S		323.9	4.57	35.99
	40S		323.9	9.53	73.88
	80S		323.9	12.70	97.47
350	5S		355.6	3.96	34.34
	10S		355.6	4.78	41.36
	40S		355.6	9.53	81.33
	80S		355.6	12.70	107.40

Note: Table values taken from ASME (2004 and 2004a). The reader will recall that STD=standard thickness pipe, XS=extra strong pipe, XXS=extra-extra strong pipe.

The second stage of regeneration is a more complete regeneration of the cryopump, to remove air and water vapor (N_2, O_2, H_2O, HTO, DTO, HDO, D_2O, T_2O, etc.). The second stage regeneration would occur perhaps once every one or two weeks during ITER shutdowns. The mass of gas released from each cryopump is expected to be small. Hauer (2007) discussed the safety requirement of keeping each cryopump below 12 moles (or 12 g of elemental hydrogen) of hydrogen gas. The pump regeneration takes about 150 seconds, so the average flow rate is on the order of < 0.1 mole/s. The regeneration gases are cryogenic cold, and the low mass quickly warms from the pipe walls to room temperature at the gas pressure of 2,000 Pa (150 Torr). When the pipe is not operating in regeneration, the gas pressure in the regeneration line is expected to be about 10 Pa (≈0.1 Torr). The cryopump foreline conditions are approximate values. The pressure in the foreline is probably on the order of 1-10 Pa (≈0.01 to 0.1 Torr) and the pipe remains near or at room temperature. The cryostat foreline is expected to be an even more benign environment than the regeneration line.

In normal operation, the regeneration pipe remains at approximately room temperature (assumed to be 20-25°C). The pipe would be baked out periodically, at least annually. The bakeout temperature would be approximately 80 to 100°C, which at the ≈2 kPa or lower gas pressure is more than adequate to mobilize any water vapor that has condensed or otherwise adhered to the pipe walls. The mobilized water vapor would be drawn to the torus exhaust processing (TEP) system.

The pipe would be monitored for its oxygen concentration. If the oxygen concentration of gas in the pipe were above the normal low levels that occur during cryopump regeneration, then the procedure would prohibit subsequent regeneration operations. In that way, any additional oxygen in the pipe would not mingle with any of the hydrogenic species that could be released from the cryopumps. The hydrogenic species would remain adhered to the pump and would not pre-mix with air or oxygen in the pipe; therefore, no gas explosion hazard would exist in the pipe.

4.3 Safety Issues with ITER Vacuum Piping

A concern from the ITER safety team was that the vacuum piping which contains hydrogen species be protected against room air inleakage. Air inleakage to low pressure piping would introduce copious oxygen that would allow formation of a hydrogen-oxygen gas mixture. There are a number of potential ignition mechanisms for such a combustible gas mixture, despite the modest temperature of the gases. Ignition mechanisms include the discharge of electrostatic charge built up from flowing gas (that is, the air rushing into the vacuum line), the beta particle energy released from tritium decay, or possibly electrical energy from instrumentation mounted on the piping for monitoring the system.

Another safety issue is that this piping is an extension of the vacuum vessel, which is a primary containment boundary for ITER radiological inventories (the in-vessel tritium and activated dusts and gases) and toxicological inventories (notably the in-vessel beryllium, and other metal dusts). As part of the containment boundary the piping is required to retain its leak-tight integrity in all situations, including normal operational stresses (e.g., vibration, bakeout thermal stresses), off-normal stresses from plasma disruptions, and the special case of the safe shutdown earthquake. The piping must be robust against these stresses.

Applications of stainless steel piping in nuclear fission power plants have given some insights about stainless steel pipe weaknesses. Pressurized water reactor (PWR) feedwater piping has suffered from high and low-cycle fatigue, erosion-corrosion, and stress corrosion cracking (Shah, 1993). Shah mentioned that feedwater piping has conditions of erosion-corrosion, flow stratification, thermal shock, water hammer (severe fluid pressure pulsations), flow induced vibration, and machinery-induced vibration. Feedwater piping has flow velocities of 3 to 7.6 m/s, with the higher velocities leading to erosion-corrosion. Shah also described issues with intergranular stress corrosion of the heat sensitized material adjacent to welds in boiling water reactor 304 and 316 stainless steels. The heat caused precipitation of chromium carbide and depletion of chromium along the grain boundaries of the alloy. The aggressive coolant environment and high residual stresses in the piping led to stress corrosion cracking, with through-wall cracks. These cracks were repaired with much plant downtime, cost, and personnel radiation exposure. Other experiences have shown that stainless steel is susceptible to halogen corrosion, especially by chlorides, which cause pitting corrosion. Most of these susceptibilities are not present in the ITER application.

4.4 General Piping Reliability Values

The best basis for a pipe failure rate value is statistical calculations using data from operating experiences of piping in the same operating conditions (or similar piping in similar conditions) as the system under study. Other approaches to obtain failure rates are computer simulations of fracture mechanics to predict failure probability of piping (Simola, 2004) and expert judgments of pipe reliability (Tregoning, 2008). All three of these approaches are used, depending on the piping design or system that the analyst must address. In this case, piping data are investigated since there are good compilations of these data available in the literature.

The piping failure rate databases that are calculated from pipe operating experience have come from two industries, the oil and gas pipelines (e.g., Vieth, 1996) and the nuclear fission power plants (Fleming, 2006). Of these two industries, the power plant piping is closer in size (diameter and wall thickness) and material (stainless steel versus carbon steel) to the ITER design. Natural gas pipelines are typically carbon steel, can vary from tens of cm to over a meter in diameter, and operate at modest temperatures (< 100°C) and pressures (≈6 MPa). Nuclear fission power plant feedwater piping can be stainless steel, on the order of 250 mm diameter, and operate at up to ≈280°C, 4.8 to 6.8 MPa water (Lobner, 1990). Granted, the flow media in power plants is high pressure water rather than low pressure gases, and the power plant pipes operate at high temperature and high pressure. However, the power plant operating experiences include stainless steel pipe material in pipes of comparable diameter to the ITER pipes of 250 and 300 mm diametre nominal (DN). The pipe material is believed to be an important factor in inferring failure rate data due to the need to account for inherent traits and susceptibilities of each unique material.

The basic failure rates for the fission reactor stainless steel piping are given in Table 4-2. These failure rates include the pipe weld, instrumentation tap, and fitting failures as well as pipe wall failures, but do not include instrument failures to retain pressure. For ITER purposes, the pipe leakage failure mode - which is a small leak by power plant standards, often less than 50 gallons of water per minute - is considered to be a consequential vacuum leak by ITER standards, a “stop-and-fix” leak. It is expected that this sort of leak would allow copious air admission that would pose the hydrogen-air explosion concern. The mean value of stainless steel pipe leakage failure rate is 8.84E−08/foot-reactor-year and the 95% upper bound failure rate of 3.31E−07/foot-reactor-year are converted to ITER-usable values by applying the 3.28 feet/meter conversion and the use of a typical US reactor-year being 7,796 hours in a calendar year. Most US power plants have been performing at over 89% availability (Blake, 2009) in the time frame of the piping study (Fleming, 2006), so (0.89)(8760 hr/year) = 7,796 h. Therefore, the average failure rate of stainless steel fission reactor piping is 3.7E−11/hr-m with a 95% upper bound of 1.4E−10/hr-m.

Table 4-2. Pipe failure rates for fission reactor stainless steel pipe.

Failure Rate	Failure Rate Uncertainty (1/foot length-reactor year)			
	Mean value	5th percentile	Median value	95th percentile
Overall failure rate, piping greater 50 mm diameter	6.43E−07	2.73E−08	2.55E−07	2.38E−06
Feedwater SS pipe spray, piping 150 to 250 mm diameter (leakage failure mode)	8.84E−08	3.70E−09	3.49E−08	3.31E−07
Feedwater SS pipe localized flood (large leak failure mode)	5.73E−08	2.43E−09	2.28E−08	2.12E−07
Feedwater SS pipe major flood (rupture failure mode)	3.07E−08	1.25E−09	1.17E−08	1.15E−07

Data taken from Fleming (2006) Table A-52 for Pressurized Water Reactor (PWR) stainless steel feedwater piping. Fleming defined spray as cc's/minute to < 100 gallons/minute water leakage, localized flood as more than 100 but less than 2,000 gallons/minute, and major flood as > 2,000 gallons/minute effluent from the pipe.

4.5 Reliability Inference of Power Plant Piping to Vacuum Piping

Inferring pipe failure rate data from the power plant to ITER vacuum piping requires accounting for the differences in the operating environments. Pipe temperature and pressure differences must be accounted for, as well as flow and the pipe wall thickness. The pipe operating temperature, flow and wall thickness will be examined to adjust the failure rate given above to apply to the ITER stainless steel pipes. The pipe wall thickness is believed to adequately account for differences in the pipe internal pressure since wall thickness increases with increasing fluid pressure.

4.5.1 Temperature Difference

ITER piping operates at 20–25°C in operation and infrequently at 80 to 100°C during bakeout, while the power plant feedwater piping operates at over 235°C, so the power plant piping has greater thermal stress. Power plant piping is heated slowly, e.g., a maximum ΔT is typically ≈30°C/hour (Rahn, 1984) for slow and even loading and unloading of thermal stresses. ITER will heat and cool the vacuum vessel internals for bakeout at a ΔT of 5°C/hour (Chiocchio, 2009) and the entire vacuum vessel will be heated from room temperature of 20°C to 200°C within 2 days (or, > 3.75°C/hour), and cooled back to pre-pulse operating temperature within 24 hours. The power plant piping has a more severe thermal environment than the ITER design environment, so the more benign ITER environment must be accounted for in the piping failure rate.

Past data sets were reviewed to determine a multiplicative factor to be used to account for the operating temperature differences in these two piping applications. Elevated temperature not only induces thermal fatigue, but aids in corrosion as well. Arulanantham (1981) gave comparisons of high and low temperature chemical process vessels and equipment, including piping. For all equipment, the high temperature failure rate average value was 1.53E−01/year, and for low temperature equipment the failure rate average value was 1.5E−03/year. Generally, in the chemical process industry, low temperature means room temperature to under 100°C and high temperature can imply a wide range of temperatures from 200°C (API, 2008) to over 1,000°C, for equipment such as steam reformers, and even gas-fired equipment at 1,500°C or greater, such as distillation columns (Moulijn, 2001). The Arulanantham study included gas-fired equipment, so the range between low temperature and high temperature is very wide. The shape of a curve of a temperature factor is expected to be similar to other mechanical equipment, an Arrhenius curve fit (NASA, 1971). The equation for the failure rate λ would be of the form (Bentley, 1993; Ushakov, 1994):

$$\lambda \quad = \quad A \bullet \exp(-B/T) \tag{4-1}$$

where

A and B are constants and T is the operating temperature in Kelvin.

Using the two data points from Arulanantham (1981),

$$\lambda_1 \quad = \quad 1.5\text{E}{-03}\text{/year at} \approx 20 \text{ C (293 K)} \tag{4-2}$$

$$\lambda_2 \quad = \quad 1.53\text{E}{-01}\text{/year at} \approx 1500 \text{ C (1773 K).} \tag{4-3}$$

From these we can calculate the values for the two constants with the mathematical manipulation:

$$\lambda_2/\lambda_1 \quad = \quad \exp\,[B \bullet (1/T_1 - 1/T2)] \tag{4-4}$$

With the data points given above we find B=1623.39 K and then solving for A gives 0.3822/year. Thus, a reasonable curve is fit to Arulanantham's two operating experience data points at different temperatures. This curve fit is now used with the fission reactor stainless steel piping operations data to estimate the failure rate for low (room) temperature stainless steel pipe use. Using a representative value of 250°C (523 K) for the fission reactor stainless steel piping gives a new λ failure rate point on the curve, 1.71E−02/year. Then, using the 20°C failure rate as the base failure rate value, the failure rate multiplier to 250°C is 1.71E−02/yr ÷ 1.5E−03/yr, or 11.43. Therefore, on an Arrhenius curve for operating temperature dependence, the multiplier from the 20°C base value to 250°C would be on the order of 11.4. If the ITER piping operates at 20 to 25°C, and the fission power plant feedwater line operates at ≈ 250°C, the failure rate for the fission piping should be divided by a factor of 11.4 to account for the lower temperature of the ITER piping.

4.5.2 Flow and Flow Media

A typical fission feedwater pipe is flowing water at a rate of 1.8E+06 kg/hour at a velocity on the order of 6 m/s (Callaway, 2006). While several authors (Fleming, 2006; Nyman, 1997) state that austenitic stainless steel is not very susceptible to flow accelerated corrosion, the flow does place stress on the piping, and operating experience shows that stainless steel piping does have some corrosion susceptibility (Shah, 1993). The corrosion aspects of the working fluid are judged to be the most important factor of this parameter.

Particle accelerator vacuum system service experience is similar to tokamak experience and is valuable to evaluate for extrapolation to fusion systems. Bacher (1990) states that corrosion in vacuum systems of particle accelerators is not as aggressive as corrosion in other vacuum environments (e.g., semiconductor manufacturing and other industrial vacuum applications). Bacher gave three primary groups of accelerator vacuum system corrodants: atmospheric corrosion (ozone, nitrogen oxides, and halogens in the presence of atmospheric humidity), cooling system corrosion, and dry corrosion between a metal and a molten metal. The corrosion at particle accelerators that occurs with the highest frequency is corrosion within cooling water systems (Kim, 2002; Sato, 2001; Chao, 1999; Hurh, 1999). Corrosion caused by leaking water from cooling systems (Mazzolini, 2004) is mentioned, as well as a few atmospheric corrosion events (Momose, 1991; Gröbner, 1992). The Large Electron Positron (LEP) collider selected stainless steel as a bellows material due to concern over the likely formation of nitric acid; stainless steel resists corrosion by that acid (LEP, 1984). Kersevan (2001) remarked that halogen contamination after some brazing operations inside the vacuum ring allowed halogen contamination and corrosion of stainless steel and aluminum parts within the European Synchrotron Radiation Facility. This was a rare occurrence that resulted from in-system work on that accelerator and similar work is highly unlikely to occur inside the ITER machine.

Tokamak vacuum systems have exhibited some corrosion due to water cooling system leaks (Pinna, 2005) but there have not been any reported corrosion events due to the presence of, or pumping of, typical fusion gases (air, helium, water vapor, hydrogen, methane and other carbon compounds, etc.) (Cadwallader, 2003; Pinna, 2005). Cooling water has leaked into vacuum systems (Surle, 1998) but it can be removed by glow discharge and baking (Pearce, 2001). Bell (2003) noted that some sulfur hexafluoride gas used in neutral beam injectors leaked into the vacuum vessel of the JET machine. This gas was unwelcome in the tritium cleanup system but apparently did not pose a concern for the vacuum components despite the fluorine halogen in that chemical compound.

The flow rate is much different for ITER piping than fission reactor piping. For the case of hydrogen species flowing in the Torus Cryopump forelines the mass flow rate on average would be 12 mols per 150 s (continuously pulsed as valves open and close) or an average of 0.08 mol/s at 2 kPa. The water flow rate in fission piping is 1.8E+06 kg/hr, or 5E+05 g/s at 8 MPa. Water is 18 g/mol, so converting to mol/s yields ≈2.8E+04 mol/s water flow rate for the fission reactor piping. This is a difference of roughly six orders of magnitude, meaning flow induced corrosion and erosion are greatly reduced.

Given that operating experiences show that corrosion inside fusion and accelerator vacuum systems is a rare event, the failure rate for stainless steel piping to be used in vacuum lines must reflect that fact. To identify a multiplier value, the stainless steel corrosion occurrences will be factored out of the fission piping failure rate. Fleming (2006, page 3-16) shows that 83% of the failure mechanisms for pipe faults in the feedwater and condensate systems of fission reactors are due to flow accelerated corrosion phenomena (e.g., pinhole leaks, wall thinning). Fusion operations experience shows this mechanism is not a dominant contributor for low flow rate vacuum piping. Vacuum piping is not susceptible to flow accelerated corrosion, so a multiplier of 0.2 (or accounting for only 20% of the fission piping failure mechanisms) will be applied to the failure rate to remove these types of failures and adjust the piping failure rate for application to fusion vacuum usage.

4.5.3 Pipe Wall Thickness

The fission feedwater pipe wall thickness is typically pipe schedule 40 (the carbon steel piping in that system is schedule 80 but the stainless steel pipe is schedule 40). From Table 4-1 for DN 300 pipe, the wall thickness is 10.31 mm for schedule 40. To account for pipe of a lesser wall thickness, the Thomas Method (Thomas, 1981) is used in a manner mentioned by Moosemiller (2006). In early risk work in the 1980's and 1990's, the Thomas method gave good results for estimating the failure rate of piping (e.g., Johnson, 1988; Medhekar, 1993) and it has been used more recently as well (Vinod, 2004; AlSalamah, 2006). In the late 1990's when more data from piping operating experiences were compiled and analyzed, the risk assessment community has decided that the Thomas method should be secondary to experience data (Lydell, 2000). However, when little or no operating experience data have been compiled, the Thomas Method is still a valid approach for piping failure rate estimation.

The Thomas Method gives the pipe leakage failure rate as being proportional to length, diameter, and wall thickness:

$$P_{leak} \alpha [L \bullet D]/t^2 \quad (4\text{-}5)$$

where

L = length of pipe

D = diameter of pipe

T = thickness of pipe wall.

Thomas states that for prevailing pipe fabrication technology, the pipe has fewer, but larger size flaws as the pipe wall thickness increases. In general, the pipe failure rate decreases as the wall thickness increases (Fleming, 2006). If the pipe length and diameter are held constant and the change in the pipe leakage probability is sought for two different pipe wall thicknesses, then the ratio of Leak Probability for thickness 1 (P1) to thickness 2 (P2) is

$$P_1/P_2 = [(L_1 \bullet D_1)/t_1^2]/[(L_2 \bullet D_2)/t_2^2] \quad (4\text{-}6)$$

The length L and diameter D are constant and cancel out of the equation, leaving

$$P_1/P_2 = t_2^2/t_1^2 \quad (4\text{-}7)$$

Therefore, if the Leak Probability 1, P_1, applies to the ITER vacuum pipe at schedule 20 (6.3 mm wall thickness), and Leak Probability 2, P_2, applies to the stainless steel fission piping at 10.31 mm wall thickness, the multiplier to apply to the fission piping failure rate is

$$(10.31 \text{ mm})^2/(6.3 \text{ mm})^2 = 2.7$$

If ITER uses pipe schedule 10, with a 4.57 mm wall thickness, the multiplier is 5.1.

4.6 Failure Rate Calculation for Vacuum Piping

The basic failure rate was taken from fission reactor operating experience since the correct type of pipe material was used and the pipe material is believed to be a very important aspect of the piping failure rate. The environmental conditions were assessed and multipliers were generated to alter the fission failure rate to apply to ITER vacuum piping. The results are given in Table 4-3.

The pipe run information is given in Figure 4-1. The resulting failure rates in Table 4-3 can be used for both the 250 DN and 300 DN piping. The torus cryopump regeneration foreline is 300 DN and 160 m length. The time of concern is assumed to be an entire year, because nitrogen atmosphere remote maintenance sessions are infrequent in the vacuum vessel and the cryopumps would probably have hydrogenic species collected on their panels over for the entire year, or 8760 hours per year. The annual failure probability of a schedule 20 pipe leaking air into the line would be

$$(1.8\text{E}{-}12/\text{hr-m})(160 \text{ m})(8760 \text{ hr/year}) = 2.5\text{E}{-}06/\text{year} \quad (4\text{-}8)$$

The other calculated values are given in Table 4-4.

Table 4-3. Failure rates and modifiers for ITER vacuum system piping.

Failure Rate and Failure Mode from Fleming (2006)	Operating Temperature Multiplier	Flow and Flow Media Multiplier	Pipe Wall Thickness Multiplier	Resulting Value for ITER Use (1/hour-m)
Mean leakage failure rate 3.7E−11/hr-m	÷11.4	× 0.2	× 2.7 for schedule 20	1.8E−12
Upper bound leakage failure rate 1.4E−10/hr-m	÷11.4	× 0.2	× 2.7 for schedule 20	6.6E−12
Mean leakage failure rate 3.7E−11/hr-m	÷11.4	× 0.2	× 5.1 for schedule 10	3.3E−12
Upper bound leakage failure rate 1.4E−10/hr-m	÷11.4	× 0.2	× 5.1 for schedule 10	1.3E−11

Table 4-4. Annual vacuum pipe leakage frequencies for ITER vacuum piping.

Failure Rate Value (/hr-m)	Annual Time (h)	Pipe Length (m)	Mean ITER Leakage Frequency per Year
Torus cryopump regeneration line, DN 300, Schedule 20 λ_{mean}=1.8E−12	8760	160	2.5E−06 (9.3E−06 ub)
Cryostat foreline, DN 250, Schedule 20 λ_{mean} =1.8E−12	8760	100	1.6E−06 (5.8E−06 ub)
Torus cryopump regeneration line, DN 300, Schedule 10 λ_{mean}=3.3E−12	8760	160	4.6E−06 (1.8E−05 ub)
Cryostat foreline, DN 250, Schedule 10 λ_{mean}=3.3E−12	8760	100	2.9E−06 (1.1E−05 ub)
Note: ub stands for the statistical 95% upper bound.			

The failure frequencies per year in Table 4-4 must be compared to some standard to determine if the frequency is acceptable. The ITER team has several definitions of normal operations, incidents, accidental situations, and hypothetical events in the Project Requirements document (Chiocchio, 2009, section 7.2). The ITER Accident Analysis Report lower frequency limit for accidental situations is 1E−06/year, which is also the upper limit for hypothetical events (also called ultimate safety margin events, or beyond design basis accidents) (Taylor, 2009). Reference event V3 is an accident event, a loss of vacuum due to vacuum line failure (this is called a dry event due to the fact that a cooling water breach does not initiate the accident). A large leak of air into the vacuum vessel followed by a hydrogen deflagration or detonation is a beyond design basis event (Taylor, 2009, section 3.3.5). The two vacuum lines discussed here are two long runs of vacuum pipe but are only a part of the total amount of piping whose failure could lead to a loss of vacuum accident event. The frequency range of accidents is not well defined in the presently available ITER documentation, but incidental events are defined as events that could occur once or more during the lifetime of the ITER plant. If the ITER lifetime is 20 years, an incidental situation occurring is a frequency of 1/20 years = 5E−02/year or greater. Therefore, the next frequency category, accidental events, is rather wide at perhaps ≈1E−02 to 1E−06/year. Therefore, these two schedule 20 pipe failures at 2.5E−06/yr + 1.6E−06/yr in Table 4-4 sum to 4.1E−06/yr, which resides near the lower limit of the accident events frequency range and are believed to not greatly change the frequency of the loss of vacuum accident event. For schedule 10 piping, the sum is 4.6E−06/yr + 2.9E−06/yr or 7.5E−06/yr, which is also close to the 1E−06/yr lower bound for design basis accidents. The frequency of leakage failure of these two single-walled pipes at either schedule 20 or schedule 10 wall thicknesses should be acceptable to the ITER project.

Some qualitative features to increase ITER pipe reliability were uncovered during this analysis. Schweitzer (2003) states that the most weldable austenitic stainless steels are those in the 200 and 300 series. An important issue in welding is that chromium carbide precipitation (sensitization) occurs under weld heat and this leads to intergranular corrosion. The sensitization can be minimized by using low carbon content or a stabilized grade of stainless steel. Preheating is not required but post-heating welds is necessary to re-dissolve the precipitated carbides and to relieve stresses. Even though stainless steel is corrosion resistant, corrosion can be initiated by surface imperfections in stainless steel. Imperfections include weld splatter, weld slag from coated electrodes, arc strikes, weld stop points, and heat tint. Weld splatter and slag should be cleaned to remove crevice-like imperfections. The ITER Vacuum Handbook is in agreement with this action since removing crevice-like features is good vacuum practice (Worth, 2008). Weld runout tabs might be feasible to preclude weld start and stop point defects. Weld contamination can be cleaned preferably by abrasive disks and flapper wheels (rather than grinding wheels) to preserve the surface (Schweitzer, 2003).

Stainless steels are susceptible to chloride (or fluoride) corrosion. Often, the chlorides are an impurity in the process fluid, but ITER fluids should have very low chloride content. However, it is known that fluorides have been an impurity in tokamaks due to the use of sulfur hexafluoride electrical insulation gas (Bell, 2003); fortunately these leaks have not caused any concerns with stainless steel corrosion. A possible countermeasure for fluoride corrosion is the use of a trap (Viola, 1992). A source of chlorides besides the process fluid is leaching from insulation materials that are often wrapped around the pipework (ASTM, 2008). If pipe thermal insulation is required, then it must be chosen to avoid halogen elements.

4.7 Conclusions

Stainless steel piping failure rates from power plants were modified for application to ITER vacuum piping. The resulting failure rates were given in Table 4-3. These failure rates were evaluated for the two pipe schedules under consideration. The frequency of leakage failure of the torus cryopump regeneration line and the cryostat foreline single-walled vacuum pipes at either schedule 20 or schedule 10 wall thicknesses should be acceptable to the ITER project.

4.8 References

AlSalamah, 2006. M. J. AlSalamah, E. Shayan, M. Savsar, "Reliability analysis of a cooling seawater pumping station," International Journal of Quality and Reliability Management, 23 (2006) 670-695.

API, 2008. Steels for Hydrogen Service at Elevated Temperatures and Pressures in Petroleum and Petrochemical Plants, seventh edition, API recommended practice 941, American Petroleum Institute, August 2008.

Arulanantham, 1981. D. C. Arulanantham and F. P. Lees, "Some Data on the Reliability of Pressure Equipment in the Chemical Plant Environment," International Journal of Pressure Vessels and Piping, 9 (1981) 327-338.

ASME, 2004. Stainless Steel Pipe, ASME B36.19M-2004, American Society of Mechanical Engineers, New York, 2004.

ASME, 2004a. Welded and Seamless Wrought Steel Pipe, ASME B36.10M-2004, American Society of Mechanical Engineers, New York, 2004.

ASTM, 2008. Standard Test Method for Evaluating the Influence of Thermal Insulations on External Stress Corrosion Cracking Tendency of Austenitic Stainless Steel, ASTM C692, ASTM International, West Conshohocken, PA, USA, 2008.

Bacher, 1990. J. P. Bacher and N. Hilleret, "Corrosion of accelerator vacuum systems: risks and prevention," Vacuum, 41 (1990) 1914-1916.

Bell, 2003. A. C. Bell, C. A. Gentile, R. L. K. Lässer, J. P. Coad, "Tritium inventory control-the experience with DT tokamaks and its relevance for future machines," Fusion Engineering and Design, 66-68 (2003) 91-102.

Bentley, 1993. J. P. Bentley, An Introduction to Reliability and Quality Engineering, Longman Science & Technical, Essex, UK, 1993, section 3.3.2.

Blake, 2009. E. M. Blake, "U.S. capacity factors: Can older reactors keep up the pace?," Nuclear News, 52 (May 2009) 29-33.

Cadwallader, 2003. L. C. Cadwallader, P. I. Petersen, "Confinement Reliability Estimates for Vacuum System Components," Fusion Science and Technology, 44 (2003) 382-387.

Callaway, 2006. Callaway Plant Final Safety Analysis Report, revision OL-15, AmerenUE Company, St. Louis, Missouri, May 2005, Chapter 10, Table 10.4-6.

Chao, 1999. A. W. Chao, M. Tigner, Handbook of Accelerator Physics and Engineering, World Scientific Publishing Co., Singapore, 1999, section 5.8.

Chiocchio, 2009. S. Chiocchio, Project Requirements (PR), ITER project document 27ZRW8, version 4.5, October 7, 2009, sections 4.2.6 and 7.1.

Day, 2006. C. Day, A. Antipenkov, I.-R. Cristescu, M. Dremel, G. Federici, H. Haas, V. Hauer, A. Mack, D. K. Murdoch, M. Wykes, "Hydrogen inventories in the vacuum pumping systems of ITER," Fusion Engineering and Design, 81 (2006) 777-784.

Fleming, 2006. K. N. Fleming and B. Lydell, Pipe Rupture Frequencies for Internal Flooding PRAs, revision 1, EPRI-TR-1013141, Electric Power Research Institute, Palo Alto, CA, 2006.

Gröbner, 1992. O. Gröbner, "Design and performance of the LEP vacuum system at CERN," Vacuum, 43 (1992) 27-30.

Hauer, 2007. V. Hauer, J.-C. Boissin, Chr. Day, H. Haas, A. Mack, D. Murdoch, R. Lässer, M. Wykes, "Design of the ITER torus prototype cryopump," Fusion Engineering and Design, 82 (2007) 2113-2119.

Hurh, 1999. P. G. Hurh, N. Kubantseva, M. P. May, "Microbiologically Influenced Corrosion in the Fermilab Main Injector Magnet Low Conductivity Water System," Proceedings of the 1999 Particle Accelerator Conference, March 29-April 2, 1999, New York, New York, IEEE, 1999, 1423-1425.

Johnson, 1988. D. H. Johnson et al., The High Flux Isotope Reactor Probabilistic Risk Assessment, final report, PLG-0604, Pickard, Lowe, and Garrick, Inc., January 1988.

Kersevan, 2001. R. Kersevan, "Vacuum system of the ESRF: operational experience and status report," Vacuum, 60 (2001) 95-99.

Kim, 2002. K. R. Kim, S. J. Kwon, S. H. Kim, Y. J. Park, H. G. Kim, K. W. Suh, S. H. Nam, C. W. Chung, and W. Namkung, "Reliability and Maintenance of PLS LINAC Mechanical Systems," Proceedings of LINAC2002, August 26-30, 2002, Gyeongju, Korea, available at: http://accelconf.web.cern.ch/AccelConf/

LEP, 1984. LEP Design Report, Volume II, The LEP Main Ring, CERN-LEP/84-01, European Organization for Nuclear Research, June 1984, section 8.4.9.

Lobner, 1990. P. Lobner, C. Donahue, and C. Cavallin, Overview and Comparison of U.S. Commercial Nuclear Power Plants, Nuclear Power Plant System Sourcebook, NUREG/CR-5640, SAIC-89/1541, Science Applications International Corporation, San Diego, CA, September 1990, chapters 3, 4.

Lydell, 2000. B. O. Y. Lydell, "Pipe failure probability – the Thomas paper revisited," Reliability Engineering and System Safety, 68 (2000) 207-217.

Mazzolini, 2004. F. Mazzolini, L. Rumiz, J. Miertusova, F. Pradal, "Ten years of ELETTRA vacuum system experience," Vacuum, 73 (2004) 225-229.

Medhekar, 1993. S. R. Medhekar, D. C. Bley, W. C. Gekler, "Prediction of Vessel and Piping Failure Rates in Chemical Process Plants Using the Thomas Model," Process Safety Progress, 12 (1993) 123-126.

Momose, 1991. T. Momose, H. Ishimaru, "Radiation damages in TRISTAN vacuum systems," Journal of Vacuum Science and Technology A, 9 (1991) 2149-2157.

Moosemiller, 2006. M. Moosemiller, "Avoiding pitfalls in assembling an equipment failure rate database for risk assessments," Journal of Hazardous Materials, 130 (2006) 128-132.

Moulijn, 2001. J. A. Moulijn, M. Makkee, A. van Diepen, Chemical Process Technology, John Wiley & Sons, Inc., Chichester, 2001, chapter 5.

NASA, 1971. Saturn Component Failure Rates and Failure Rate Modifiers, NASA TM X-64619, accession number N72-13416, December 1971.

Nyman, 1997. R. Nyman, D. Hegedus, B. Tomic, B. Lydell, Reliability of Piping Systems, Framework for Estimating Failure Parameters from Service Data, third edition, SKI 97:26, STATENS KÄRNKRAFTINSPEKTION, Stockholm, Sweden, December 1997. Available at: http://www.stralsakerhetsmyndigheten.se/Global/Publikationer/SKI_import/050112/346f84543ce49119ba04ebb69cfb6d57/1997_26_3rd.pdf

Pearce, 2001. R. Pearce, J. Bruce, S. Bryan, N. Green, J. Orchard, S. Scales, "Vacuum integrity and protection systems at JET," Vacuum, 60 (2001) 137-145.

Pinna, 2005. T. Pinna, G. Cambi, S. Ciattaglia, A. Lo Bue, S. Knipe, J. Orchard, R. Pearce, and U. Besserer, "Collection and analysis of data related to fusion machines (JET and TLK) operating experience on component failure," Fusion Engineering and Design, 75-79 (2005) 1199-1203.

Rahn, 1984. F. J. Rahn, A. G. Adamantiades, J. E. Kenton, D. Braun, A Guide to Nuclear Power Technology, John Wiley & Sons, Inc., New York, 1984, chapter 12.

Sato, 2001. H. Sato, T. Kubo, K. Marutsuka, Y. Saito, M. Shirakata, and N. Tokuda, "Experience of the erosion-corrosion problems in the main ring cooling water system at the KEK-PS," Proceedings of the 2001 Particle Accelerator Conference, June 18-21, 2001, Chicago, Illinois, IEEE, 2001, 1426-1428.

Schweitzer, 2003. P. A. Schweitzer, Metallic Materials, Physical, Mechanical, and Corrosion Properties, Marcel Dekker, Inc., New York, 2003, pp. 99-104.

Shah, 1993. V. Shah, P. E. MacDonald, editors, Aging and Life Extension of Major Light Water Reactor Components, Elsevier, Amsterdam, 1993, chapters 2, 5, 15, 19.

Simola, 2004. K. Simola, U. Pulkkinen, H. Talja, P. Karjalainen-Riokonen, A. Saarenheimo, "Comparison of approaches for estimating pipe rupture frequencies for risk-informed in-service inspections," Reliability Engineering and System Safety, 84 (2004) 65-74.

Surle, 1998. F. Surle, G. Mayaux, M. Chantant, J. Malagoli, D. Monbrun, P. Patier, B. Thos, "The Tore Supra Cooling System: 10 years of operation," Fusion Technology 1998, Proceedings of the 20th Symposium on Fusion Technology, Marseille, France, September 7-11, 1998, Association Euratom-CEA, 1998, 665-668.

Taylor, 2009. N. Taylor, Accident Analysis Report (AAR), Volume I – Event Identification and Selection, ITER project document ITER IDM 2DPVGT, version 1.3, November 2009.

Thomas, 1981. H. M. Thomas, "Pipe and Vessel Failure Probability," Reliability Engineering, 2 (1981) 83-124.

Topilski, 2009. L. Topilski, S. Reyes, Accident Analysis Report – Volume III, Hypothetical Event Analysis, ITER project document ITER_D_2E2XAMv.4.1, May 6, 2009.

Tregoning, 2008. R. Tregoning, L. Abramson, P. Scott, Estimating Loss of Coolant Accident (LOCA) Frequencies Through the Elicitation Process, NUREG-1829, US Nuclear Regulatory Commission, Washington, DC, April 2008.

Ushakov, 1994. I. A. Ushakov, R. A. Harrison, Handbook of Reliability Engineering, John Wiley & Sons, Inc., New York, 1994, page 433.

Vieth, 1996. P. H. Vieth, I. Roytman, R. E. Mesloh, J. F. Kiefner, Analysis of DOT Reportable Incidents for Gas Transmission and Gathering Pipelines – January 1, 1985 through December 31, 1994, American Gas Association, task NG-18, report 213, catalog number L51745, May 1996.

Vinod, 2004. G. Vinod, H. S. Kushwaha, A. K. Verma, A. Srividya, "Optimisation of ISI interval using genetic algorithms for risk informed in-service inspection," Reliability Engineering and System Safety, 86 (2004) 307-316.

Viola, 1992. M. Viola, L. Dudek, V. Garzotto, J. Kemperschroer, G. Martin, R. Rossmassler, and R. Sissingh, "SF6 and Water Cold Trap for TFTR Deuterium-Tritium Operations," Proceedings of the 14th Symposium on Fusion Engineering, San Diego, CA, September 30 – October 5, 1991, IEEE (1992) 1004-1007.

Worth, 2008. L. Worth, ITER Vacuum Handbook, Appendix 13, "Guide to Cleaning and Cleanliness for the ITER Project," ITER Project document ITER_D_2ELUQH_v1_1, January 12, 2008.

5. COPPER TUBING JOINT RELIABILITY

On May 19, Mr. C. Hamlyn-Harris of the ITER IO vessel division inquired about copper joint reliability. The cryogenics designers were preparing for a design comparison review of ITER thermal shield designs. An important point to address was the joint reliability of copper-copper joints and steel-steel joints. The joint in question contains gaseous helium at 80 K and 1.8 MPa, and resides in a vacuum environment in the cryostat. Mr. Hamlyn-Harris requested failure rate data on copper joints and on copper to stainless steel joints.

While this query is directed to cryogenic system joints, the data from the TFTR magnet coil joints was believed to give a long-lived, high population count data set on copper joints and would serve as a comparison value against cryogenic system operating experience data found to address the joint reliability question.

5.1 TFTR Operating Experiences

A general source of copper-copper joint information is the joint connections in the toroidal field magnets of the Tokamak Fusion Test Reactor (TFTR). While these are not cryogenic joints, they do serve as an independent data point for comparison purposes. As always with operating experience failure rates, three values are needed: the operating time, the number of components, and the number of failed components.

5.1.1 TFTR Operating Time

The TFTR operated from December 24, 1982 to April 4, 1997 (Machalek, 1983; von Halle, 1998). The typical approach used in data analysis for tokamaks at this time is to count not just the pulse seconds but to count the preparation time, the pulse seconds, and the post-pulse recovery time (diagnostic data archiving, machine cooldown, and machine configuration for the next pulse). This is because the systems are active and operating over that entire time interval. The TFTR stated that in initial operation the quickest it could recover from a plasma pulse was 300 seconds (5 minutes) when removing magnet heat. After the TF magnet water coolant conversion to fluorinert in May 1993, the coil cooldown time was lengthened to 900 seconds (15 minutes) (Barnes, 1994; Barnes 1995; Walton, 1994). Over its lifetime, TFTR produced more than 80,000 high power plasmas (von Halle, 1998). No data were found to properly partition the pulse counts in the D-D and D-T operating periods, so a yearly average of pulses was assumed. TFTR operated for 14.25 years, with an average of 80,000/14.25 = 5,600 pulses per year. In the 1983 to early 1993 time frame (10.33 years), the operation time per pulse was 5 minutes. So the run time in that time partition is estimated to be (5,600 pulse/y)(10.33 y)(5 min/pulse) giving 289,240 minutes or 4,820 hours. In late 1993 to 1997 (3.92 years) the operation time per pulse was 15 minutes. The run time was (5,600 pulse/y)(3.92 y)(15 min/pulse) giving 329,280 minutes, or 5,488 hours. The total hours would be 4,820+5,488 = 10,308 hours of operation. This would be a conservatively low estimate since the tokamak would not necessarily pulse as quickly as the magnets had cooled. The pulse count estimate of 80,000 high power pulses does not include the machine conditioning plasmas, or the test plasmas where the magnets were used, but the high power plasmas would have stressed the toroidal field magnets more than the other types of pulses.

5.1.2 Number of Components

TFTR design data show that there were 20 TF coils in use on the tokamak (Smith, 1977), and that there were 44 copper-copper joints within each coil. The copper-copper joints had an extra provision for reliability of using a copper sleeve piece inside the copper-copper joint as an additional barrier to prevent leakage (Heitzenroeder, 1991). The copper conductor was Copper Development Association 104 material specification (UNS C10400), an oxygen free (0.001% oxygen maximum) high conductivity copper with 0.027% silver as an alloying element. There were on the order of 1,500 linear feet (457 m) of hollow copper conductor wound into one coil, and the copper conductor weighed 14 short tons or 12,700 kg per coil (Sabado, 1984). Figure 5-1 shows a sketch of the conductor, which came in three thicknesses (0.558, 0.607, and 0.683 inches) and one width, 6.547 inches. The three thicknesses were used to help balance the temperature in the coil. The conductor sections were about 35 feet long. The TF magnet coils were held to a maximum temperature of 150°F (65.6°C) during pulse operations due to concerns about insulation integrity and material strength. The water coolant entered at 50°F (10°C) and each coil had a flow of 150 gallons/minute (Smith, 1977).

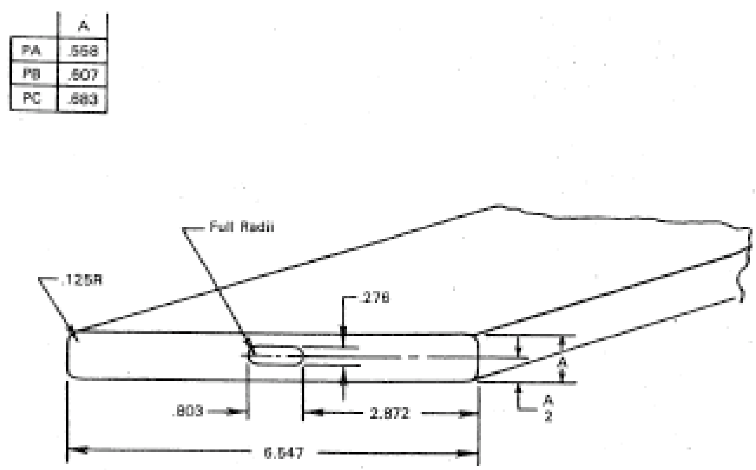

Figure 5-1. Sketch of the TFTR hollow copper conductor.
Notes: This sketch was taken from Tobias, 1979. Dimensions are given in inches, the coolant opening is 0.803 inch width by 0.270 inch height.

The joints in the conductor were made by induction brazing (Tobias, 1979). The American Welding Society braze alloy BCuP-5, a 15% silver, 5% phosphorous, and 80% copper alloy, was used as the filler material. This brazing filler alloy is identified as UNS C55284. As mentioned by Heitzenroeder (1991) this filler is self-fluxing and no additional external flux was used in the braze. Water-cooled chill blocks were used during brazing to minimize the heat-affected zone of the braze. The joints were made carefully, with attention to detail and inspections of the work (Tobias, 1979). A set of 25 pre-production samples were braze joined to demonstrate the ability to meet the joint quality requirements and to perfect the technique. Joint preparation included fashioning a 60° vee joint, followed by surface preparation and cleaning (Tobias, 1979). Joint testing was carried out for each conductor joint by pressurizing the passage with helium and sniffing with a mass spectrometer while the joint was under tension from a hydraulic apparatus in a hydraulic test fixture (Heitzenroeder, 1991). Electrical conductivity was also checked.

5.1.3 Fault Events

TFTR documented several events with the toroidal field magnets. Heitzenroeder (1991) mentioned that the TF coils had several instances of water leakage within the coils. At least two leaks were the results of cracks in oval copper tubing, which was additional coolant tubing brazed into the outer edge of a TF coil turn. That coolant tubing outside the TF coils was extruded as a continuous length.

Zatz (2003) discussed coil examinations during the TFTR dismantling process for final disposal. One examination was of coil #18, which had exhibited a chronic leak of the lead spur joint within the body of the coil. This spur joint for water coolant had a leak that defied all repair attempts during coil life. Coil #3 had developed several leaks in the fourteen water fittings at the base of the coil. The coil #3 leaks were the motivation to change coolants from de-ionized water to fluorinert. Zatz stated that several TF coil bundles which were cut from magnet coils #3 and #18. When those TF coil bundles were being separated for metallurgical investigation, several turns had visibly detectable brazed joints where the lengths of copper conductor were spliced to form the wound coil. Every inspected joint had a flawless appearance and no evidence of wear or residual defect. Other, more cursory inspections of other coils also showed no joint integrity concerns. Inspection revealed that the copper in the immediate vicinity of the brazed joints was softer than typical conductor copper. This softer, lower strength copper region was attributed to the idea that the high temperatures employed during the brazing process had locally annealed the copper. This effect had been anticipated in the coil design, the brazed joints were intentionally staggered by design to avoid a concentration of annealed copper in the coil windings. The brazed joints were designed to be stronger than the local copper, and all but one yield test specimen failed in the copper rather than in the brazed joint. From this evidence it would appear that none of the TFTR TF copper conductor brazes leaked. Given the high amount of care taken in joint cleaning, preparation and fabrication, joint testing, and the close spacing nature of the joints wound into the coils, the assumption of no joint failures is not surprising.

This assumption does raise the question of where did cooling water leak from TFTR magnets? Zatz (2003) described the investigation of the water fittings on the sides of the TF coils. There were 14 fittings on each coil that routed water in and out of the coil, connecting to cross wise cooling channels machined into a conductor. Several of these water fittings were the cause of the water leaks that plagued the TF coils. There were two leaks in TF coil #3 and one leak in TF coil #18. Zatz investigated these water fittings and determined that the probable cause was that the crosswise channels were severely deformed and were not all centered in the thickness of the conductor turn, leaving a thin wall of copper. There were through cracks in the turn. The reasoning based on this evidence was that deformation during manufacturing and then brazing the water fitting to the copper plate lead to locally annealed copper in the crosswise channel. When the conductor was wound into the coil turn, buckling could occur in the areas with thin walls.

Statistical calculations for both the copper conductor joint brazes and the water fitting brazes are performed below.

5.2 Statistical Calculations for TFTR Data

Focusing on the copper joint brazes in the TFTR hollow conductor, there were 44 brazes in each coil, for a total of 44x20 = 880 braze joints. Each braze was of a section 16 cm long across the face of the conductor (see Figure 5-1). There were 10,308 hours of operation assumed. Assuming no failures based on the coil examination evidence, the average failure rate would be $\lambda = 0.5/T$, where T is the total operating time of the set of components (Atwood, 2003). Therefore, the average λ is 0.5/(880 joints)(10,308 hours) or 5.5E−08/joint-hour. Rounding off would give 6E−08/joint-hour. This failure rate would be applied to any failure mode, including small and large leakage, rupture, or blockage. The upper and lower bounds are calculated by the Chi-square distribution. An upper bound failure rate (Atwood, 2003) with a 95% Chi-square distribution and 2n+2 degrees of freedom (where n=number of failure events) is $\chi^2(0.95,2)/2T$. The $\chi^2(0.95,2)=5.99$ as found from Chi-square tables in O'Connor (1985). The upper bound failure rate calculation is (5.99)/(2)(880 joints)(10,308 hours) or 3.3E−07/unit-hour. Rounding off this value would give 3E−07/unit-hour. The Chi-square 5% lower bound failure rate calculation with 2n+1 degrees of freedom would be (0.103)/(2)(880 joints)(10,308 hours), or 5.7E−09/unit-hour. Rounding off this value would give 6E−09/unit-h.

The other failure rate of interest is the copper water fittings to each TF coil. There were 14 fittings on each coil, for a total of 280 brazed fittings. The operating time is the same as given above, 10,308 hours. There were three known failures that were a combination several conditions: improper wall thickness of the crosswise water channel, the braze heat-affected zone softening of the copper, and the winding stresses in the copper conductor that overstressed the weakened, thin wall (Zatz, 2003a). The average failure rate would be λ = n/T where n is the number of failures and T is the total operating time of the set of components. In this case, n=3 leaks and T=280 x 10,308 h. Therefore, $\lambda_{leakage}$ = 3/(280 joints x 10,308 hours) or 1E−06/fitting-hour. The 95% upper bound Chi-square value for 2n+2 degrees of freedom would be 15.5/2(280)(10,308 h) or 2.7E−06/unit-hour. Rounding would give 3E−06/unit-hour. The 5% lower bound with 2n degrees of freedom would be 1.64/2(280)(10,308 h) or 2.8E−07/unit-hour. Rounding off would give 3E−07/unit-hour.

5.3 Additional Joint Data

Mr. Hamlyn-Harris provided some other data on hypervapotron units used on the Joint European Torus (JET) neutral beam injectors (NBIs). A hypervapotron sketch is given in Figure 5-2. These rectangular hypervapotrons are built of a copper chrome zirconium alloy (CuCrZr) and have an electron beam weld to join the 2 CuCrZr plates. The electron beam welds were performed in a vacuum environment. There are 200 hypervapotrons in service on JET and each one has approximately 2 meters of longitudinal e-beam weld. None of these weld joints have been reported to leak in service over the entire NBI operating life thus far. The hypervapotron cooling water is 5 bar, 20°C, and flows at a velocity of 3.75 m/s. Outside the hypervapotron is vacuum at the conditions kept for the NBIs. The hypervapotrons also have water line stainless steel to CuCrZr joints that are brazed. There are approximately 440 of these joints in service, and there have been two leakage failures documented due to poor brazes (Milnes, 2007).

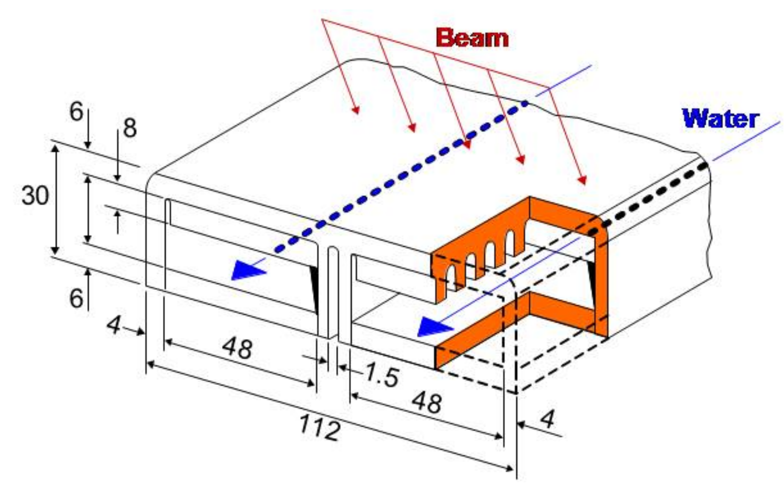

Figure 5-2. Sketch of a JET NBI hypervapotron.
Notes: This figure was taken from Milnes, 2007. Dimensions are in mm.

With this component definition and failure count, the operating time is needed. The JET NBI components have been in operation for ≈25 years; that is, through 2007 when the report giving the failure counts was published. JET began operation on June 25, 1983 (Green, 1989) and remains in operation today. While the water coolant flows for about 50% of each year, the NBI presently operates for one plasma pulse every thirty minutes between 0600 and 2200 hours, six days a week for 6 months per year. That is approximately 16 operating hours per operating day, 6 days/week and 24 weeks a year or a possible 2304 operating hours per year. Since the hypervapotrons are heated during the pulse and returned to normal temperature during the dwell time between pulses, this is the time of highest stress and it is used for the failure rate calculations. It is known that fusion experiments do not achieve every pulse attempted, thus a multiplier will be used to estimate the number of successful JET pulses where it is expected that heat loading on the hypervapotrons has occurred. Ciattaglia (2005) gave some data for JET that showed about a 90% ratio of successful pulses to total pulses attempted. This multiplier will be used in the time calculation. It is also noted that Pinna (2007) showed the NBI system was not a mature operating system until 1988, that the NBI experienced over 90 failures in the first 3.5 years of operations then the count of failures per year reduced to only 1 or 2. However, since the hypervapotrons have not been listed as failing, the entire time duration can be counted as the service life of these units rather than 'early life' with high numbers of failures and then 'mature component lifetime' with low numbers of failures.

Green (1989) discussed that JET did not always operate in two shift operations from 0600-2200 hours per operating day. In 1983-1984 JET operated in single shift operations, usually 10-hour days, 60 hours/week. In 1985, double shift operating days of 16 hours were commenced. From 1983-1987, Green gave operating day counts of 42, 75, 155, 229, and 133.5, respectively. From 1988 and on, the data from Mr. Hamlyn-Harris have been used to estimate the operating hours. Table 5-1 gives the annual operating hours estimates. These are only estimates; it is well known that tokamak operations vary due to outages for modifications, annual funding levels for electrical power, outages for repairs, etc.

The failure rate for the e-beam weld of CuCrZr material is calculated per meter-operating hour. Atwood (2003) gives the failure rate, λ, for no observed failures as λ=0.5/T, where T is the total component operating hours. In the case of electron beam welds, T=(200 hypervapotrons)(2 meters e-beam weld/hypervapotron) (49,977 hours of operation). Therefore, λ=0.5/1.999E+07 m-h or 2.5E−08/m-h. Rounding up gives 3E−08/m-h. This is an "all modes" failure rate since no specific mode of failure has manifested itself for this e-beam weld. An upper bound failure rate (Atwood, 2003) with a 95% Chi-square distribution and 2n+2 degrees of freedom (where n=number of failure events) is $\chi^2(0.95,2)/2T$. The $\chi^2(0.95,2)=5.99$ as found from Chi-square tables in O'Connor (1985). The upper bound failure rate calculation is (5.99)/(2)(1.999E+07 m-h) or 1.5E−07/unit-hour. Rounding off this value would give 2E−07/unit-hour. The Chi-square 5% lower bound failure rate calculation with 2n+1 degrees of freedom would be (0.103)/(2)(1.999E+07 m-h), or 2.6E−09/m-h. Rounding off this value would give 3E−09/m-h. The average failure rate of 3E−08/m-h is the same order of magnitude as some other published information on conventional welds, such as 7E−08/h-m for small leaks (Bünde, 1991), although Bünde's estimation value for e-beam welds gives a small leakage failure rate of 7E−09/h-m. Schnauder (1997) gave an analyst consensus failure rate estimate for electron beam welds of 1E−09/m-h. These two estimates were both lower values than the calculated failure rate. Welds and piping tend to be special cases in reliability; analysts seek very large populations over long operating times to give pipe and weld operating experience failure rates. It is possible that since there have been no failures in these e-beam welds that longer operating times will give lower values, but these JET data produce a good failure rate for no failure events over the time interval. Operating experience data supercede judgments unless there are compelling reasons to the contrary. It should be noted that the most prevalent failure mode of welds in piping applications is small leakage of process fluid. This mode is considered to be the primary failure mode being considered when “all modes” values are discussed for welds. The calculated “all modes” weld failure rate would, in

Table 5-1. JET annual operating hours estimates.

Calendar year	Operating hours per day	Operating days per year	Operating hours per year
1983	10	42	420
1984	10	75	750
1985	16	155	2480
1986	16	229	3664
1987	16	133.5	2136
1988	16	144	2304
1989	16	144	2304
1990	16	144	2304
1991	16	144	2304
1992	16	144	2304
1993	16	144	2304
1994	16	144	2304
1995	16	144	2304
1996	16	144	2304
1997	16	144	2304
1998	16	144	2304
1999	16	144	2304
2000	16	144	2304
2001	16	144	2304
2002	16	144	2304
2003	16	144	2304
2004	16	144	2304
2005	16	144	2304
2006	16	144	2304
2007	16	144	2304
Total			55,530 hours

Note: Using the 90% factor to account for poor or failed pulses that did not heat the hypervapotrons gives 49,977 operating hours over the time period.

theory, apply to small leakage, large leakage, and rupture failure modes. Eventually some form of failure would occur in the component population that would define a specific failure mode.

The hypervapotrons also have two stainless steel to CuCrZr joints for connecting water lines. Out of the approximately 440 joints in service, 2 have failed by small water leak due to insufficiently wetted joint surfaces when brazing the joints. The failed joints appeared to be wetted adequately at the time of brazing but time in service revealed inadequacies. The average failure rate would be $\lambda = n/T$ where n is the number of failures and T is the total operating time of the set of components. In this case, n=2 leaks and T=440 joints x 49,977 hours. Therefore, $\lambda_{leakage}$ = 2/(440 joints x 49,977 hours) or 9.1E−08/joint-hour. Rounding off gives 9E−08/joint-hour. The 95% upper bound Chi-square value for 2n+2 degrees of freedom would be 12.6/2(440)(49,977 h) or 2.9E−07 per joint-hour. Rounding off gives 3E−07/joint-hour. The 5% lower bound failure rate with 2n degrees of freedom would be 0.711/2(440)(49,977 h) or 1.6E−08/joint-hour. Rounding up gives 2E−08/joint-hour.

Literature searches were conducted but did not reveal any additional data. The discussions of cryogenic systems used in aerospace activities, at particle accelerators, and in industry did not contain enough detail to develop the three pieces of data necessary to calculate a failure rate. Searches on the term “dissimilar metals” gave discussions on joining processes and case histories, and some insight to the issues of joint metallurgy: differences in thermal expansion and heat capacity of two metals, discussions of galvanic corrosion of dissimilar metals, and other topics, but no quantifiable failure rate data.

5.4 Conclusions

Table 5-2 gives the results of the calculations performed here. The failure rates of the Tore Supra cryogenic system stainless steel-aluminum friction joints calculated in Section 3 are also given in the table for comparison. It is noted that the average failure rates for all of these joining methods are the same order of magnitude at 1E−08 per joint-hour with the exception of the TFTR water fittings. Those water fittings were noted to have had several issues that decreased their reliability. The conductor braze joints did not suffer from these issues, and regardless of the type of usage, their failure rates range from 6E−08/h to 9E−08/h, which is a rather consistent set of failure rate data from diverse equipment and materials – magnet copper conductor Cu-Cu brazed joints and CuCrZr-stainless steel brazed joints. The cryogenic SS-Al friction joint failure rate was 5E−08/h, which is quite comparable to the brazed joint values.

Since the TFTR copper conductor joints were not repairable amid the coil windings, making solid joints was important to machine success. There was a high level of pre-fabrication testing to develop a reliable braze process, specialized equipment was set up to carry out the braze process, operators were trained and care was used in the braze process, and there was a high level of quality assurance during the process as well. A number of tests were carried out to verify joint reliability before and after winding the coil pancakes of their magnets. A tested fabrication process, careful work and inspections led to high braze reliability (Tobias, 1979). These steps allowed the magnet conductor brazes to perform without failure over the ≈14 year life of TFTR and gave the low failure rate calculated here. The Tore Supra cryogenics system personnel stated these same ideas when discussing the success of having no joint failure events within the cold boxes of the Tore Supra cryogenic system.

Table 5-2. Results of failure rate estimates.

Component	Failure Mode	Average Failure Rate	95% Upper Bound Failure Rate	5% Lower Bound Failure Rate
Cu-Cu brazed joints in TFTR TF magnets	All modes	6E−08/joint-h	3E−07/joint-h	6E−09/joint-h
Cu water fitting brazes in TFTR TF magnets	Small leakage	1E−06/fitting-h	3E−06/fitting-h	3E−07/fitting-h
CuCrZr e-beam welds in JET hypervapotron	All modes	3E−08/m-h	2E−07/m-h	3E−09/m-h
CuCrZr to stainless steel brazes in JET hypervapotron water lines	Small leakage	9E−08/joint-h	3E−07/joint-h	2E−08/joint-h
SS-Al cryogenic friction joints from Tore Supra cryogenic system	Small leakage	5E−08/joint-h	3E−07/joint-h	3E−09/joint-h

5.5 References

Atwood, 2003. C. L. Atwood, J. L. LaChance, H. F. Martz, D. J. Anderson, M. Englehardt, D. Whitehead, T. Wheeler, *Handbook of Parameter Estimation for Probabilistic Risk Assessment*, NUREG/CR-6823, US Nuclear Regulatory Commission, Washington, DC (September 2003) page 6-6.

Barnes, 1994. G. W. Barnes, G. R. Walton, D. Bashore, "Operation of a Fluorinert Cooling System for the TFTR TF Coils and TFTR Coil Flowswitch Monitoring System Modification to Accommodate the TF Alternate Cooling System (Fluorinert)," *Proceedings of the 15th Symposium on Fusion Engineering*, Hyannis, MA, October 11-15, 1993, IEEE (1994) 329-332.

Barnes, 1995. G. W. Barnes, R. Pysher, J. Chrzanowski, R. Woolley, "Operation of a Fluorinert Cooling System for the Toroidal Field Coils on TFTR," *Proceedings of the 16th Symposium on Fusion Engineering*, Champaign, IL, September 30-October 5, 1995, IEEE (1995) 520-521.

Bünde, 1991. R. Bünde, S. Fabritsiev, and V. Rybin, "Reliability of welds and brazed joints in blankets and its influence on availability," *Fusion Engineering and Design*, **16** (1991) 59-72.

Ciattaglia, 2005. S. Ciattaglia, B. M. Angelini, M. Cox, O. Grüber, D. van Houtte, K. Kurihara, P. Petersen, M. de Baar, P. Sonato, "Availability of Present Fusion Devices," *Proceedings of the 21st Symposium on Fusion Engineering*, Knoxville, TN, September 26-29, 2005, IEEE (2005) compact disk proceedings, MFE Engineering oral session.

Green, 1989. B. J. Green, P. Chuilon, B. Noble, R. Saunders, D. Webberley, "Machine Utilisation and Operation Experience with JET from 1983," *Fusion Technology 1988, Proceedings of the 15th Symposium on Fusion Technology*, Utrecht, The Netherlands, 19-23 September, 1988, North-Holland Publishers, Amsterdam, 1989, 1633-1637.

Heitzenroeder, 1991. P. J. Heitzenroeder, "Designing Magnetic Systems for Reliability," PPPL-CFP-2469, CONF 910968-30, Princeton Plasma Physics Laboratory, January 1991.

Machalek, 1983. M. D. Machalek, "First Plasma Operation of TFTR," *Nuclear Technology/Fusion*, **4** (1983) 191-193.

Milnes, 2007. J. Milnes, B. Chuilon, *JET Neutral Beam – Recent Structural Integrity Issues*, CD/E&CG/T/086, UKAEA Fusion, September 12, 2007.

O'Connor, 1985. P. D. T. O'Connor, *Practical Reliability Engineering*, second edition, John Wiley & Sons, Publishers, New York (1985) appendix 3.

Pinna, 2007. T. Pinna, G. Cambi, and F. Gravanti, "Collection and analysis of component failure data from JET systems: neutral beam injectors and power supply," *Nuclear Fusion*, **47** (2007) S453-S457.

Sabado, 1984. M. Sabado, R. Little, "TFTR Materials Issues and Problems During Design and Construction," *Journal of Nuclear Materials*, **122&123** (1984) 1087-1098.

Schnauder, 1997. H. Schnauder, C. Nardi, M. Eid, "Comparative availability analysis for the four European DEMO blanket concepts in view of the selection exercise," *Fusion Engineering and Design*, **36** (1997) 343-365.

Smith, 1977. G. E. Smith, W. F. B. Punchard, "TFTR Toroidal Field Coil Design," *Proceedings of the 7th Symposium on Engineering Problems of Fusion Research*, Knoxville, TN, October 25-28, 1977, IEEE (1977) 15-19.

Tobias, 1979. J. B. Tobias, "Brazing of Large Section Water-Cooled Copper Conductor on TFTR," *Proceedings of the 8th Symposium on Engineering Problems of Fusion Research*, San Francisco, CA, November 13-16, 1979, IEEE, (1979) 117-123.

von Halle, 1998. A. von Halle and the TFTR Group, "Final Operations of the Tokamak Fusion Test Reactor (TFTR)," *Proceedings of the 17th Symposium on Fusion Engineering*, San Diego, CA, October 6-10, 1997, IEEE (1998) 65-69.

Walton, 1994. G. R. Walton, A. Brooks, A. Harnsberger, H. Murray, J. Satkofsky, "Design of the TFTR TF Coil Alternate Cooling System," *Proceedings of the 15th Symposium on Fusion Engineering*, Hyannis, MA, October 11-15, 1993, IEEE (1994) 325-328.

Zatz, 2003. I. J. Zatz, *TFTR D&D Project: Final Examination and Testing of the TFTR TF-Coils*, PPPL-3777, Princeton Plasma Physics Laboratory, January 2003.

Zatz, 2003a. I. J. Zatz, "Final Examination and Testing of the TFTR TF-Coils," *Proceedings of the 20th Symposium on Fusion Engineering*, San Diego, CA, October 14-17, 2003, IEEE, (2003) 31-34.